[American Journal of Science, Vol. 302, February, 2002, P. 110–143]

AN INTEGRATED ASSESSMENT OF A "TYPE EUXINIC" DEPOSIT: EVIDENCE FOR MULTIPLE CONTROLS ON BLACK SHALE DEPOSITION IN THE MIDDLE DEVONIAN OATKA CREEK FORMATION

JOSEF P. WERNE*, BRADLEY B. SAGEMAN**, TIMOTHY W. LYONS***, and DAVID J. HOLLANDER****

ABSTRACT. An integrated lithologic, paleontologic, and multi-proxy geochemical study of the Middle Devonian Oatka Creek Formation, a black shale in the northern Appalachian Basin, indicates that a number of different factors contributed to organic carbon-rich black shale deposition. Conditions leading to this organic-rich sedimentary deposit were ultimately controlled by a relative sealevel rise, dominantly eustatic but with possible contributions from local tectonics, which cut off the supply of carbonate to the basin. Geochemical proxy evidence – such as Mo/Ti, Fe/Ti, C_{org}, S_{py}, and $\delta^{34}S_{py}$ – suggests that as sealevel continued to rise after the carbonate supply was cut off, a threshold was crossed at which point conditions in the basin shifted from dominantly anoxic to dominantly euxinic (anoxic-sulfidic bottom waters). Concurrent with the shift to dominantly euxinic conditions, the supply of siliciclastic sediments was cut off, resulting in a condensed horizon, as evidenced by the elemental ratios of Si/Al and K/(Fe+Mg) and the relative concentration of eolian silt as determined petrographically and from scanning electron microscopy. Sediment starvation in the basin appears to have facilitated the biogeochemical (re)cycling of C, N, and P. Specifically, the elemental ratios of C, N, and P and the stable carbon isotope composition of organic matter suggest that the preferential regeneration of P under anoxic conditions (and of N during the oxic phase of oxic/anoxic oscillation) led to enhanced primary production in surface waters, thereby maintaining euxinic conditions in the bottom waters through respiration of settling organic matter. Finally, it is observed that, though conditions in the basin seem to have remained consistently anoxic-sulfidic for some time after the initial shift to euxinic conditions, a progressive increase in siliciclastic sedimentation led to a corresponding decrease in the enrichment of various redox-related elements, illustrating the overriding control that sedimentation can have on geochemical proxy records.

INTRODUCTION

Black shales have long been a focus of study because of their potential as hydrocarbon source rocks. More recently, the linkage between carbon cycling, organic matter (OM) burial, and global climate change has re-ignited interest in black shales as long-term carbon reservoirs and archives for biogeochemical proxies reflecting the conditions that produced them. A succession of competing models has been proposed to explain the origins and occurrence of black shale deposits. The most recent debate has focused on two endmember models to explain the organic enrichment observed in black shales: the "preservation" model (Demaison and Moore, 1980) and the "productivity" model (Pederson and Calvert, 1990). In short, the preservation model calls upon the existence of a permanently stratified, stagnant water column in which anoxic depositional conditions account for the enrichment of OM in black shales by favoring enhanced preservation relative to oxic depositional settings. Alternatively, productivity arguments suggest that high OM concentrations result from elevated primary produc-

*Department of Geological Sciences, Northwestern University, Evanston, Illinois, 60208; Present address: Large Lakes Observatory and Department of Chemistry, University of Minnesota Duluth, Duluth, Minnesota 55812
**Department of Geological Sciences, Northwestern University, Evanston, Illinois, 60208
***Department of Geological Sciences, University of Missouri, Columbia, Missouri, 65211
****Department of Marine Science, University of South Florida, St. Petersburg, Florida, 33701

tion in the overlying water column. In the productivity model, anoxic conditions are a consequence rather than the cause of organic enrichment. Although little of the available evidence from ancient deposits readily distinguishes between these two models, recent studies have suggested that the "either/or" view is flawed (Arthur and Sageman, 1994; Canfield, 1994; Murphy and others, 2000). For example, variations in rates of subsidence and relative sealevel and the subsequent changes in sediment grain size, sedimentation rate, and oceanographic circulation as well as changes in biogeochemical cycling are now recognized as important contributing factors in the accumulation of organic-rich deposits (Tyson and Pearson, 1991; Arthur and Sageman, 1994; Canfield, 1994; Hedges and Keil, 1995; Ingall and Jahnke, 1997; Murphy and others, 2000).

In this study we have employed an integrated, multi-proxy approach to study the Middle Devonian Oatka Creek Formation of the lower Hamilton Group—traditionally considered a classic example of the "preservation" endmember reflecting deposition in a stagnant, euxinic basin (Byers, 1977; Ettensohn, 1992). The large number of possible factors affecting the deposition of black shales, however, suggests that multiple dependent and independent processes (biological, physical, and chemical) may have contributed to the deposition of the Oatka Creek Formation. Here, we have integrated lithologic, paleontologic, and geochemical observations to assess the relative influences of the different processes and conditions related to the deposition of this black shale. Because most geochemical parameters are influenced by more than one process, multiple geochemical proxies are used to identify the dominant processes within a given depositional system. The data used in this study fall into three fundamental groups: (1) proxies associated with the deposition of biogenically produced carbonate, (2) proxies associated with the flux of siliciclastic materials from riverine and eolian inputs, and (3) proxies associated with the accumulation of authigenic/diagenetic mineral phases reflecting temporal and spatial variability in redox conditions and related microbial activities.

Our data suggest that the Oatka Creek Formation was deposited under euxinic conditions (anoxic, sulfidic bottom waters) but not necessarily beneath a permanent pycnocline. Furthermore, other conditions and processes contributed to the development and maintenance of euxinic conditions in the basin, such as sediment starvation, enhanced primary productivity, and biogeochemical feedbacks on nutrient cycling.

GEOLOGICAL BACKGROUND

Paleogeography, climate, tectonics, and sealevel.—The central Appalachian basin is believed to have occupied a position in the southern subtropics (15-30°S) during deposition of the Oatka Creek Formation (Witzke and Heckel, 1988; Scotese and McKerrow, 1990). Recent reconstructions place the basin in the path of easterly trade winds carrying moisture from the Iapetus Ocean, but the Acadian Orogen likely formed a major rainshadow (Woodrow, 1985) resulting in a seasonally variable, arid to semi-arid climate that was subject to intense storms (possibly monsoons) (Woodrow, Fletcher, and Ahrnsbrak, 1973; Heckel and Witzke, 1979; Scotese, Barrett, and Van der Voo, 1985; Woodrow, 1985; Witzke and Heckel, 1988; Witzke, 1990). Deposits of the Hamilton Group show abundant evidence for the influence of storm events in nearshore (Woodrow, 1985; Slingerland and Loulé, 1988; Prave, Duke, and Slattery, 1996) and offshore (Brett, Baird, and Miller, 1986; McCollom, 1988) facies.

In a series of papers, Ettensohn (1985a, b) and Ettensohn and others (1988) developed a comprehensive tectono-stratigraphic model for the Appalachian basin that synthesized many previous studies (see fig. 1). The model by Ettensohn (1985a, b) and Ettensohn and others (1988) argued for three to four major phases of southward migrating deformation in the Acadian orogeny (Boucot and others, 1964; Rodgers, 1967; Johnson, 1971). Ettensohn (1985a, b) interpreted these phases of deformation

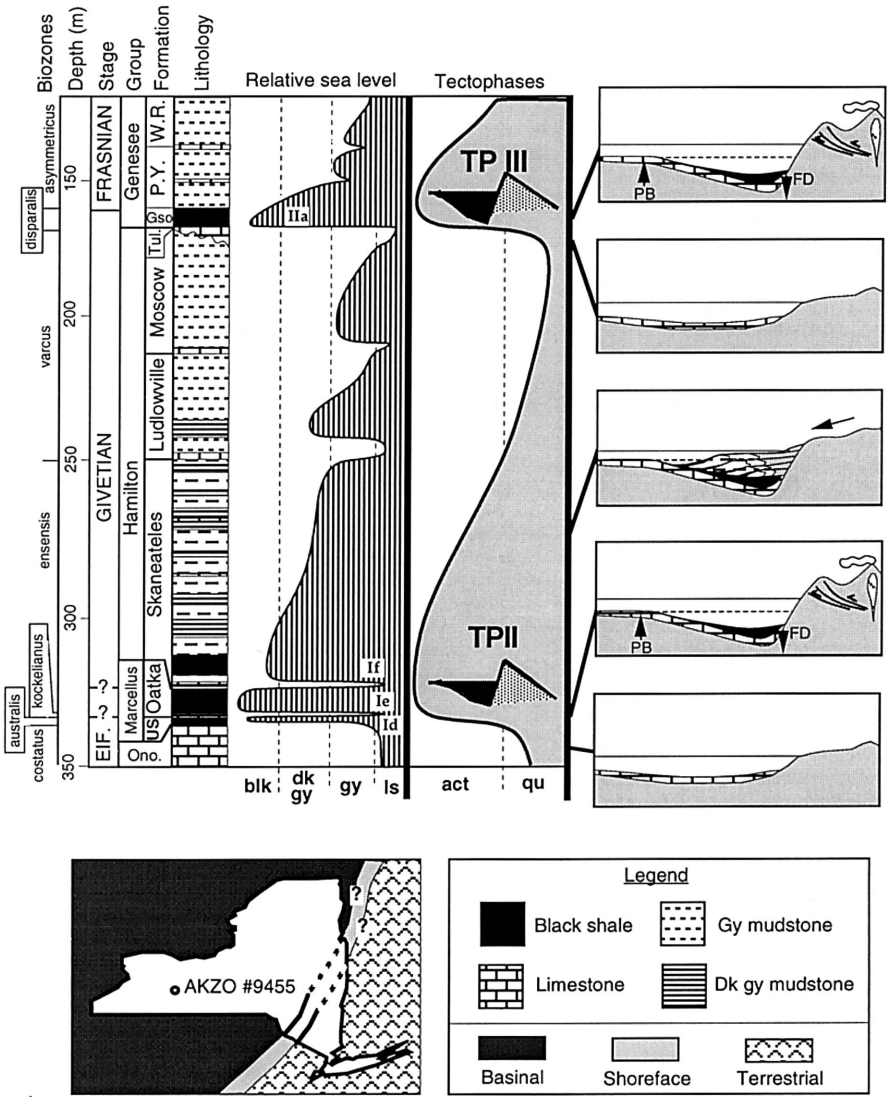

Fig. 1. Geologic setting for study of Oatka Creek Formation in Akzo core #9455: figure modified from Murphy and others (2000 and references therein) shows regional stratigraphy for Hamilton Group (Ono.=Onondaga Limestone, US=Union springs Shale, Tul.=Tully Limestone, Gso.=Geneseo Shale, P.Y.=Penn Yan Shale, W.R.=West River Shale), relative sealevel interpretation based on lithofacies (blk=black shales, dkgy=dark gray shales, ls=bioclastic limestones) and biofacies (Brett and Baird, 1994), and subsidence history based on tectophase model of Ettensohn (1985a, b) (act=active, qu=quiescent; PB=peripheral bulge, FD=foredeep; dashed line in cross sections indicates pycnocline). The map on lower left illustrates inferred paleoshoreline and generalized facies belts for early Givetian time relative to New York State outline (based on Woodrow, 1985; Dennison, 1985); transition from solid to dashed shoreline marks limit of preserved Devonian strata. Biozones from Klapper (1981) and Klapper and Johnson (1990). Eustatic rise events (Id through IIa) of Johnson and Sandberg (1988).

as tectono-stratigraphic cycles of subsidence in the foreland basin (Quinlan and Beaumont, 1984) followed by filling of the basin with sediments as the uplifted orogen was eroded. In this model the shales are the deep-basin equivalents of the Catskill Delta complex. Each cycle, or tectophase, of Ettensohn (1985a, b) and Ettensohn and others

(1988) is represented by a distinctive stratigraphic sequence characterized by shallow-water carbonates overlain by transgressive black mudstones, deposited under anoxic conditions beneath a "nearly permanent" pycnocline, such as the Oatka Creek Formation. These black shales are in turn overlain by increasingly clastic-rich units ranging from sandstones in proximal areas to gray mudrocks in more distal areas, ultimately covered by carbonate rocks (Ettensohn, 1985a, b; Ettensohn and others, 1988). The comprehensive framework of this model (fig. 1) links the large-scale tectonic history of the Appalachian basin with an oceanographic-sedimentologic mechanism to account for high accumulation of OM in units like the Oatka Creek Formation. Although the general relationships remain applicable, alternative interpretations for two major aspects of the model should be reconsidered in light of more recent work.

The first alternative interpretation of the model concerns Acadian orogenesis and its relationship to basin subsidence, sealevel, and stratigraphic architecture. Hamilton-Smith (1993) noted that a relatively conformable section spanning from the Onondaga Limestone into the lower Hamilton Group (fig.1) argues against a peripheral bulge uplift associated with Oatka Creek deposition, thereby weakening the case for tectonically driven subsidence at this time as originally proposed by Ettensohn (1985a,b) and Ettensohn and others (1988). Alternatively, a eustatic sealevel rise documented at the Eifelian-Givetian boundary (Hallam, 1984; Johnson and Sandberg, 1988) could account for increasing accommodation and deposition of the Oatka Creek black shale. The evidence for tectonic influence on basin subsidence is much stronger for Tectophase III (corresponding to deposition of the Geneseo Shale, fig. 1; Hamilton-Smith, 1993), yet a eustatic rise is also interpreted for this event (Hallam, 1984; Johnson and Sandberg, 1988). Although these observations of combined tectonic-eustatic controls are consistent with Ettensohn's (1985a,b) conclusion that the Geneseo Shale represents a deeper stratified basin than the Oatka Creek Formation, recent results contradict this view (Murphy and others, 2000).

The second major challenge to the Ettensohn model concerns water-column stratification. Despite the absence of direct observational evidence confirming the presence of a "nearly permanent" pycnocline in the basin as proposed by Ettensohn (1985a), water-column stratification has been a solid fixture in the Devonian literature since the 1970's. For example, Byers (1977) used the Black Sea as a depositional analog for euxinic basins. Baird and Brett (1986) produced the only indirect observations in support of a pycnocline when they interpreted winnowed zones on the basin margin to reflect the erosive effects of internal waves that propagated along the pycnocline and ultimately intersected the seafloor; however, such features are inadequately explained and quite limited in stratigraphic occurrence. In recent years, the Black Sea-based pycnocline model, once the favored interpretation for most epeiric black shale deposits, has been increasingly questioned due to: (1) the difficulty inherent in sustaining water-column stratification in open marine systems, especially in light of evidence for frequent mixing by storms; (2) the recognition that in modern marine environments the most common cause of density stratification is the temporary development of a seasonal thermocline rather than permanent stratification (Tyson and Pearson, 1991); and (3) evidence suggesting that OM accumulation may be due to enhanced productivity rather than stable stratification (Pedersen and Calvert, 1990). A major objective of the present study is to investigate alternative hypotheses for enhanced OM burial in black shale facies of the Appalachian Basin.

Lithostratigraphy and biostratigraphy.—The Oatka Creek Formation, one of the most organic carbon-rich units in the Middle to Upper Devonian section of western New York, appears conformable in the study area. This unit is part of a thicker black shale interval (the Marcellus Formation) that constitutes the basal Hamilton Group and early Tectophase II (figs. 1 and 2). A recent revision of the stratigraphic nomenclature

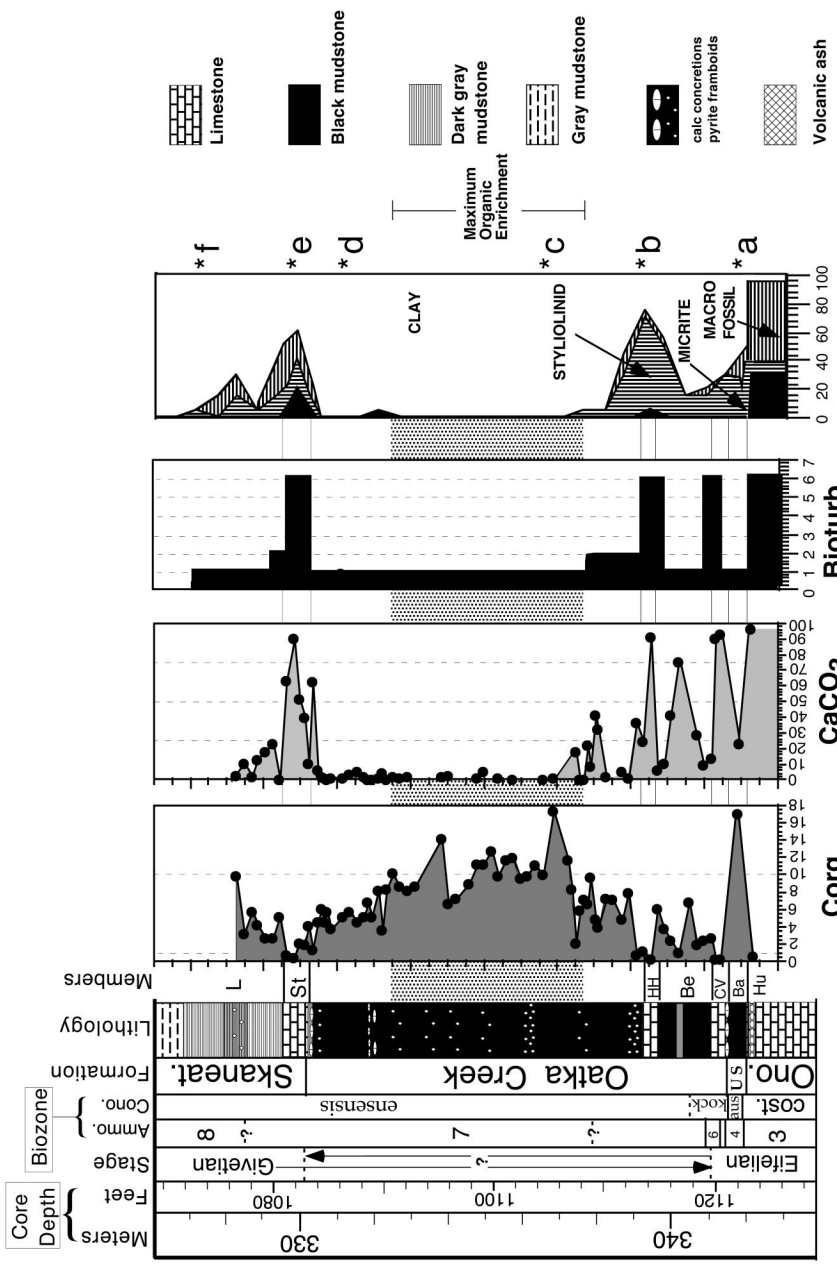

Fig. 2(A). Lithostratigraphy, biostratigraphy, C_{org} percent, $CaCO_3$ percent, bioturbation (ichnofabric rank), particle type, and thin sections from Oatka Creek Formation. Zone of maximum organic enrichment (MOE) is marked by gray background. Pyrite framboids increase in concentration in MOE. Asterisks indicate the interval from which thin sections were taken. Abbreviations are Bakoven Mbr (Ba), Halihan Hill Bed (HH), Cherry Valley Limestone (CV), Berne Mbr (Be), Hurley Mbr (Hu).

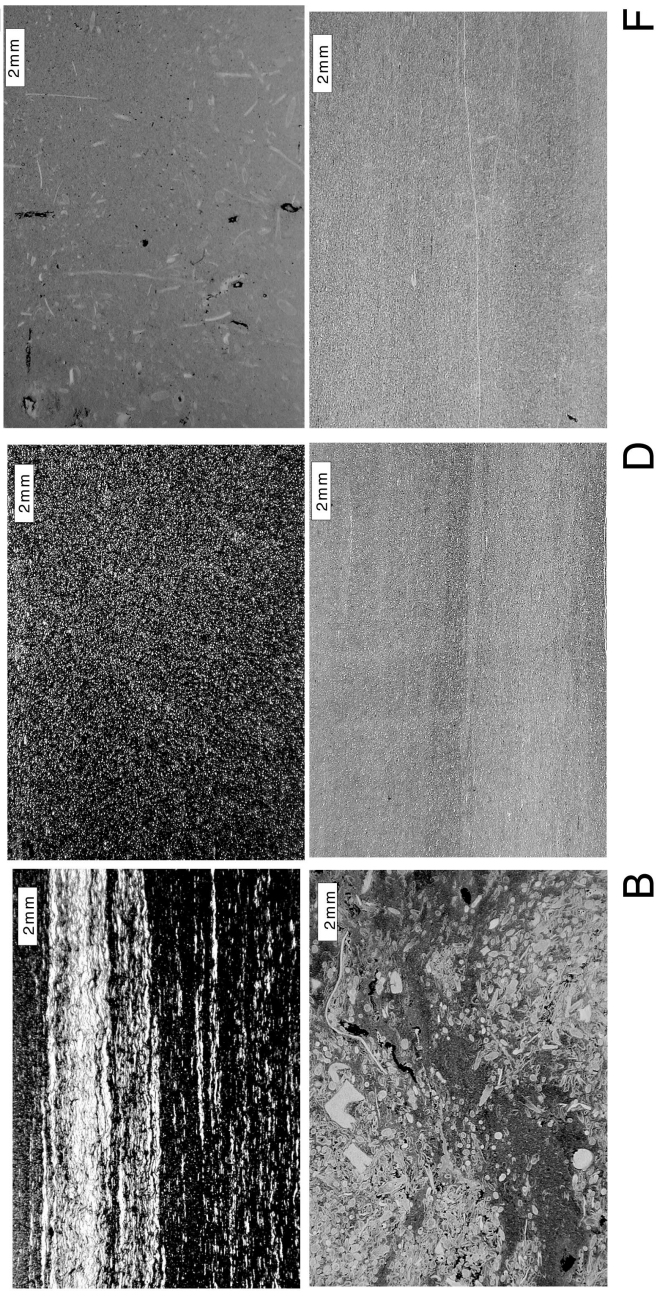

Fig. 2(B). Thin sections (A) styliolinid shell hash forming lamination in sulfidic black mudstone of Ba; (B) carbonate of HH; (C) taken in MOE, C_{org}, and pyrite maxima, also maximum silt concentration (small white grains); (D) black mudrock just above MOE, showing decreasing pyrite and silt content; (E) carbonate of Stafford Member (St); (F) overlying Skaneateles Formation dark gray mudstone, showing significantly decreased concentration of both pyrite and silt grains.

for this region by Ver Straeten, Griffing, and Brett (1994) elevated the Marcellus Formation to subgroup status (fig. 1). The new Marcellus Subgroup directly overlies the Seneca Member of the Onondaga Limestone and includes, in ascending stratigraphic order, the Union Springs Formation and the Oatka Creek Formation (figs. 1 and 2). In Akzo core #9455 (fig. 1), the focus of the present study, the Union Springs Formation is represented by the 30 cm thick Bakoven Member, a black organic-rich mudstone, and the 10 cm thick Hurley Member, a concretionary, fossiliferous limestone horizon (figs. 1 and 2). The Hurley Member lies in sharp contact with the overlying 35 cm thick bioclastic Cherry Valley Limestone bed. The Cherry Valley Limestone is the informal basal member of the Oatka Creek Formation. It is overlain by three additional informal members: (1) the 170 cm thick Berne Member, an organic-rich mudstone; (2) the 45 cm thick Halihan Hill bed, a bioclastic limestone; and (3) the almost 9 m thick unnamed member, a highly organic-rich silty mudstone (figs. 1 and 2). The Oatka Creek Formation is directly overlain by the Skaneateles Formation, which includes a basal 50 cm thick limestone, the Stafford Member, which is overlain by dark gray, moderately organic-rich mudstones of the Levanna Member. There is no evidence for a significant unconformity at any contact, although many of these units display features of moderate to extreme condensation (for example, hardgrounds).

The interpretation of relative conformity is supported by biostratigraphic data at the level of resolution possible using conodont and ammonoid biozones. These taxa constrain the Eifelian-Givetian boundary within the Marcellus subgroup, but the exact placement of the boundary is debated (Klapper, 1971, 1981; House, 1978, 1981; Rickard, 1984; Woodrow and others, 1988; House and Kirchgasser, 1993; Kirchgasser and Oliver, 1993). Nevertheless, evidence for a complete succession of the major conodont and ammonoid indices argues against major stratigraphic gaps (figs. 1 and 2).

METHODS

Analysis of the Oatka Creek Formation was conducted on a pristine core (Akzo #9455) obtained from the Akzo-Nobel Salt Corporation, Livingston County, New York. The core was slabbed to facilitate lithologic descriptions and subsequently subsampled for petrographic and geochemical analyses. Lithologic units were described at millimeter- to centimeter-scale for physical and paleobiological characterization (rock color, lithology, sedimentary structures, ichnofabric and ichnotaxa, and identifiable macrofossils). The degree of bioturbation was recorded on a seven point scale similar to the scheme proposed by Droser and Bottjer (1986): well to moderately to poorly laminated, burrowed, and poorly to moderately to highly bioturbated; 1-7, respectively; table 1). Carbonate grain types were divided into three categories (macrofaunal skeletal material, styliolinids, and micrite/calcisilt) based on visual observation of the core face, and their abundances were estimated in terms of percent exposure in the core face surface. Ichnofauna and macrofauna were recorded at generic to species level when possible, otherwise to the lowest determinable taxonomic level. Thin sections were prepared from subsamples representing all facies within the study interval and analyzed using standard petrographic techniques. Selected thin sections were examined at magnification up to 1000x under the scanning electron microscope to characterize individual grain textures and grain surface features. Subsamples for geochemical analysis were collected at 10 to 20 cm intervals. Preparation of these samples included washing with acetone and distilled/deionized water to remove surficial contaminants associated with coring and storage, followed by crushing to $<$200 mesh. Powdered samples were then analyzed for a suite of elements and stable isotopes as follows.

TABLE 1

Ichnofabric scale for core description

Rank	Features
0 – 1	no primary fabric
1 – 2	very well laminated, no burrows
2 – 3	well laminated, rare small burrows
3 – 4	moderately laminated, small to large burrows
4 – 5	poorly laminated, small to large burrows
5 – 6	burrowed
6 – 7	bioturbated

Geochemistry

Carbon.—Concentrations of total carbon and total inorganic carbon (IC) were determined using a UIC Carbon Coulometer and bulk-sample combustion and acid digestion, respectively. The average error is less than ±1 percent. Total organic carbon (C_{org}) was determined by difference. IC was converted to percent carbonate by stoichiometric calculations assuming all inorganic carbon is present as calcium carbonate.

Carbon/nitrogen ratios.—Samples were acidified in 0.1N HCl to remove carbonate for analysis of the atomic ratios of carbon and nitrogen (N_{org}) in OM. Acidified samples were combusted using a Fisons NA 1500 Elemental Analyzer. C_{org} and N_{org} concentrations were determined from the resulting CO_2 and N_2 gases with a precision of ±2 percent.

Phosphorus.—Phosphorus concentrations were determined by a modified Aspila, Agemian, and Chau (1976) approach (Ingall, Bustin, and Van Cappellen, 1993). Inorganic phosphorus (phosphate) is determined by digestion in concentrated HCl overnight followed by UV visible spectrophotometry. Total phosphorus is measured by combustion followed by HCl digestion and spectrophotometry, and organic phosphorus is determined by difference. Reproducibility for the P concentration measurements was ±5 percent.

Sulfur.—Concentrations of reduced sulfur were determined by chromium reduction following the method of Canfield and others (1986), with a reproducibility of ±1.5 percent. The chromium reduction method is specific to total reduced inorganic sulfur (pyrite in the shales of the present study) (Canfield and others, 1986; Lyons, 1997).

Iron.—Concentrations of pyrite-Fe were calculated from reduced sulfur concentrations assuming a pyrite stoichiometry. Acid soluble Fe (HCl-Fe) was determined by digestion in boiling 12N HCl for 1 m, followed by spectrophotometric quantification

(Stookey, 1970; Raiswell, Canfield, and Berner, 1994) with a reproducibility of ±3 percent. Total Fe was determined by whole-rock elemental analysis using inductively-coupled plasma-atomic emission spectrometry (ICP) and a multi-acid digestion (Lichte, Golightly, and Lamothe, 1987).

Degree-of-pyritization (DOP).—DOP values were determined to assess iron availability and, by inference, possible relationships to the degree of bottom-water oxygenation of the depositional environment following Raiswell and others (1988) and using the equation:

$$\mathrm{DOP} = (\text{pyrite-Fe})/[(\text{pyrite-Fe}) + (\text{HCl-Fe})],$$

where pyrite-Fe and HCl-Fe are assumed to account for all the reactive Fe present in the samples. More specifically, "HCl-Fe" has traditionally been treated as the remaining unsulfidized portion of the Fe pool with the potential to react with H_2S. Traditionally, this "reactive" Fe component is delineated as the fraction of total solid-phase Fe that is readily solubilized during a boiling 12 N HCl distillation for 1 m (Berner, 1970; Raiswell, Canfield, and Berner, 1994). Recent work has shown, however, that the HCl-soluble fraction includes Fe phases requiring prolonged exposure to dissolved sulfide ($\geq 10^2$ yr and much greater in some cases) and thus is an overestimation of the most readily reactive Fe (Canfield, Raiswell, and Bottrell, 1992; Raiswell, Canfield, and Berner, 1994; Raiswell and Canfield, 1996). Furthermore, DOP varies not only as a function of depositional redox conditions but also, as will be discussed below, across temporal and spatial gradients in the rate of siliciclastic sedimentation (Canfield, Lyons, and Raiswell, 1996; Lyons, 1997; Raiswell and Canfield, 1996, 1998; Lyons, Werne, and Hollander, 2002).

Other elements.—Concentrations of other major, minor, and trace elements (Al, Ba, Ca, Cr, Co, Cu, Fe, Mg, Mo, Ni, P, K, Si, Na, Ti, V, and Zn) were quantified via ICP following multi-acid digestion (Lichte, Golightly, and Lamothe, 1987), with a precision of better than ±1 percent.

Stable carbon isotopes.—Samples were acidified in 0.1N HCl to remove carbonate carbon for analysis of the stable isotopic composition of carbon in OM ($\delta^{13}C_{org}$). Samples were then combusted using a Fisons NA 1500 Elemental Analyzer. The isotopic ratios of the resultant CO_2 gas were measured using a continuous flow inlet system linked to a Fisons Optima stable isotope mass spectrometer. Carbon isotope analyses were run in triplicate. Carbon isotope values are reported relative to the VPDB standard using the conventional permil (‰) notation. Standard deviation was generally less than 0.2 permil.

Stable sulfur isotopes.—Isotopic compositions of pyrite sulfur were measured on Ag_2S precipitates of the sulfide liberated by the chromium reduction method (Newton and others, 1995; Lyons, 1997). The Ag_2S precipitate was combusted in the presence of cupric oxide under vacuum to convert to SO_2 and analyzed on a Finnigan MAT Delta E gas source stable isotope ratio mass spectrometer. Sulfur isotopic values are reported as permil (‰) deviations from the S isotope composition of Cañon Diablo troilite (CDT) using the conventional delta ($\delta^{34}S$) notation. Sulfur isotope results were generally reproducible within ± 0.1 to 0.2 permil.

RESULTS

Lithofacies

Carbonate and mudrock lithofacies can be defined in the study interval, with subfacies distinguishable based on relative proportions of three major sedimentary components (siliciclastic mud, carbonate mud, and OM) and a group of accessory constituents (fossils, quartz silt, and pyrite).

Carbonates.—Samples with $CaCO_3$ concentrations greater than 70 percent are defined as limestones (fig. 2). Most carbonate lithotypes in the study interval fall within this category. The limestones are further divisible into a group characterized by mudstone to wackestone textures (Onondaga Limestone and Stafford Member of Skaneateles Formation) and a group with wackestone to packstone or grainstone textures (Hurley Member, Cherry Valley Limestone, and Halihan Hill bed). All limestones range from medium to light gray in color and are fossiliferous and bioturbated. Thin intervals of organic-rich siliciclastic mudstone facies have $CaCO_3$ contents in excess of 50 percent and are thus defined as marlstones. The carbonate in these organic-rich marlstones is present as abundant coarse to fine shell material and is commonly churned by bioturbation. These units appear transitional between organic-rich mudstone and carbonate lithotypes.

Mudrocks.—The mudrock facies range from noncalcareous (<10 percent $CaCO_3$) to calcareous (10-50 percent $CaCO_3$) (fig. 2). They are generally divisible into black mudstones and gray mudstones based on color, as well as C_{org} content and sediment fabric (Brett, Dick, and Baird, 1991). Black mudstones have C_{org} values ranging from 4 to 16 percent and comprise the Union Springs Formation and the unnamed member of the Oatka Creek Formation (the average C_{org} value for the unnamed member is 7.5 percent) (fig. 2). Dark gray mudstones have a C_{org} content ranging between 1 and 4 percent and are present in the Berne Member of the Oatka Creek Formation and the lower Skaneateles Formation (fig. 2). Gray mudstones (not represented by data in fig. 2) contain <1 percent C_{org} and are interbedded with dark gray mudstones throughout the Skaneateles Formation above the study interval. Because rocks in drill core lack the fissility that generally develops from the weathering of finely laminated mudrocks, use of the term "shale" is technically not appropriate. However, contrary to the expectation based on studies of other organic rich facies, the dark mudrocks of the Marcellus subgroup do not consistently display a fine, even lamination. In fact, lamination is only visible in cases where horizons of distinctive particles – such as calcareous bioclasts (styliolinids), quartz silt, or OM – define laminae (fig. 2) and are not destroyed by bioturbation. Within the core of the interval of maximum organic enrichment there is negligible carbonate content but abundant quartz silt (up to 45 percent); however, neither hand samples nor thin sections show any trace of a laminated fabric. In addition to quartz silt, the black mudrocks contain common to abundant pyrite framboids (fig. 3).

Biofacies

In this study, biofacies descriptions of the core consisted of continuous classification of ichnofabric level (see table 1, fig. 2), identification of ichnotaxa wherever possible, and identification of characteristic macrofossil taxa. Biofacies characterization allowed correlation to published descriptions of Marcellus subgroup assemblages from outcrops. In addition, observations of changes in dominant particle types through the study interval (as percent of the polished core face) provided an independent indicator of biogenic versus siliciclastic contributions (fig. 2).

In general, all carbonate beds contained evidence of diverse benthic assemblages (including crinoids, brachiopods, corals, bryozoans, and trilobites) and high levels of bioturbation (fig. 2), including *Planolites, Chondrites*, and *Zoophycos*. Mudrock biofacies ranged from moderately diverse in dark gray mudstones down to a nearly complete lack of fossil material in some horizons of the maximum organic-rich black mudstones. The unnamed member of the Oatka Creek Formation mostly contained only rare, thin *Leioryhncus* fragments and very rare styliolinid fragments. Styliolinids are commonly interpreted as a pelagic heterotroph, and although they range throughout the study interval, abundance peaks occur in the Union Springs black mudstone, the Halihan Hill bed, and the Stafford Limestone Member (fig. 2).

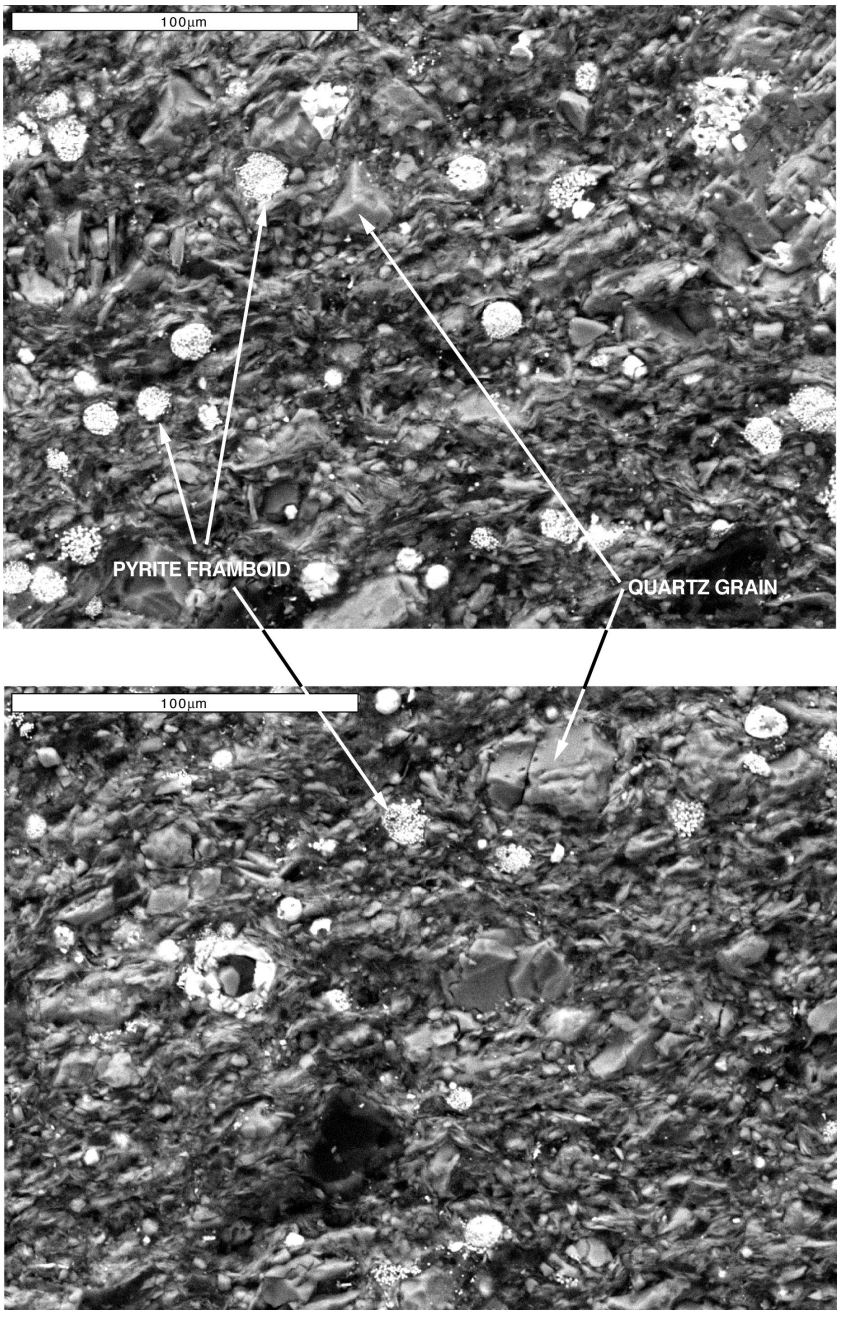

Fig. 3. Scanning Electron Microscope images of Oatka Creek Formation, taken in the MOE. Note angularity and pitting of quartz grains, and size range of pyrite framboids. Scale bars are 100 μm.

The transition from the Onondaga fauna to the Hamilton Fauna, which represents a major turnover event separating intervals of faunal stasis in the Appalachian basin, occurs within the study interval (Brett and Baird, 1995). The first appearance of

Hamilton fauna occurs within the Halihan Hill bed, and this fauna persists with only minor changes for ~6 to 10 my, up to the Geneseo Shale (Brett and Baird, 1995) (fig. 1). The faunal turnover therefore corresponds to the deposition of black mudstones in the Union Springs Formation, bioclastic limestones of the Hurley Member-Cherry Valley Limestone, and/or dark gray to black mudstones of the Berne Member.

Geochemistry

Carbon.—Generalized trends for C_{org} and $CaCO_3$ concentrations are described above in the lithofacies results. During deposition of the unnamed member of the Oatka Creek Formation (337-327 m), $CaCO_3$ wt percent is effectively zero (below detection by coulometry), with only occasional measurable quantities of less than 5 percent (fig. 2). Based on thin section analysis, the carbonate fraction includes biogenic shell material and micritic carbonate. The shell material, comprised dominantly of styliolinids with minor contributions from *Leioryhncus*, is extremely thin and does not show discernible evidence of dissolution. In the lower portion of the unnamed member, at ~337 m, there is a marked increase in C_{org} concentration to more than 17 percent, followed by a gradual upsection decline (fig. 2). There is no visible change in lithology at the C_{org} excursion. In fact, the magnitude of this C_{org} change well exceeds the increase in C_{org} observed in the transitions from bioturbated carbonate facies to organic-rich mud facies, so the change in C_{org} cannot be attributed to varying $CaCO_3$ dilution. The central portion of the unnamed member is here defined as the zone of maximum organic enrichment (MOE) based on the first and last samples to record C_{org} values of ~10 percent (essentially between 337 and 333 m depth in the core; see fig. 2).

Detrital indicators.—Below ~337 m depth in the core, the Si/Al ratio is relatively stable and low with values of about 2.5 (fig. 4). At 337 m, there is a marked increase to significantly higher values exceeding 4, followed by a gradual up-section decrease to values similar to those at the base of the section (~2.5). The ratio K/(Fe+Mg) reaches a maximum of >1 in the lower part of the section (Berne Member through lower unnamed member; up to ~337 m) (fig. 4). At 337 m, K/(Fe+Mg) suddenly decreases to ~0.35, remains low for several meters, and then gradually increases in the upper part of the core until in the upper unnamed member it reaches levels almost as high as those in the Berne Member. Finally, at the same horizon (337 m), Ti/Al drops to some of the lowest measured levels for the entire Hamilton Group.

Redox indicators.—S_{py} concentrations and Mo/Ti ratios show very similar trends (fig. 5). Both are relatively low in the Cherry Valley Limestone and the Berne Member, which are carbonate-rich units. At approx 337 m, the base of the MOE in the unnamed member, both parameters increase significantly at a horizon with no visible change in lithology. Following this excursion, both parameters decrease gradually upsection to the overlying Stafford Member of the Skaneateles Formation where values are similar to those observed below the unnamed member. DOP values in the Oatka Creek Formation are high during deposition of the lower subunits (~0.6-0.8) but increase to maximum values (~1.0) during deposition of the middle unnamed member at the same horizon as the positive excursion in Mo/Ti and S_{py}, that is, at the base of the MOE. The sulfur isotopic composition of pyrite, $\delta^{34}S_{py}$, maintains a value of approx –5 to –15 permil below 337 m, decreases abruptly by 10 to 20 permil at the base of the MOE and remains at ~–30 permil throughout the upper portion of the section.

Indicators of biogeochemical cycling.—The C_{org}/N_{org} ratio (atomic) is ~10-15 in the lower units of the Oatka Creek Formation and increases sharply to nearly 50 in the black shale of the unnamed member at the base of the MOE (fig. 6). After peaking at nearly 50, the C_{org}/N_{org} ratio decreases gradually up section until values of ~10 are reached in the uppermost Oatka Creek Formation. The C_{org}/P_{total} ratio is more variable than the C_{org}/N_{org} ratio. In the lower units, C_{org}/P_{total} ranges from near 0 to

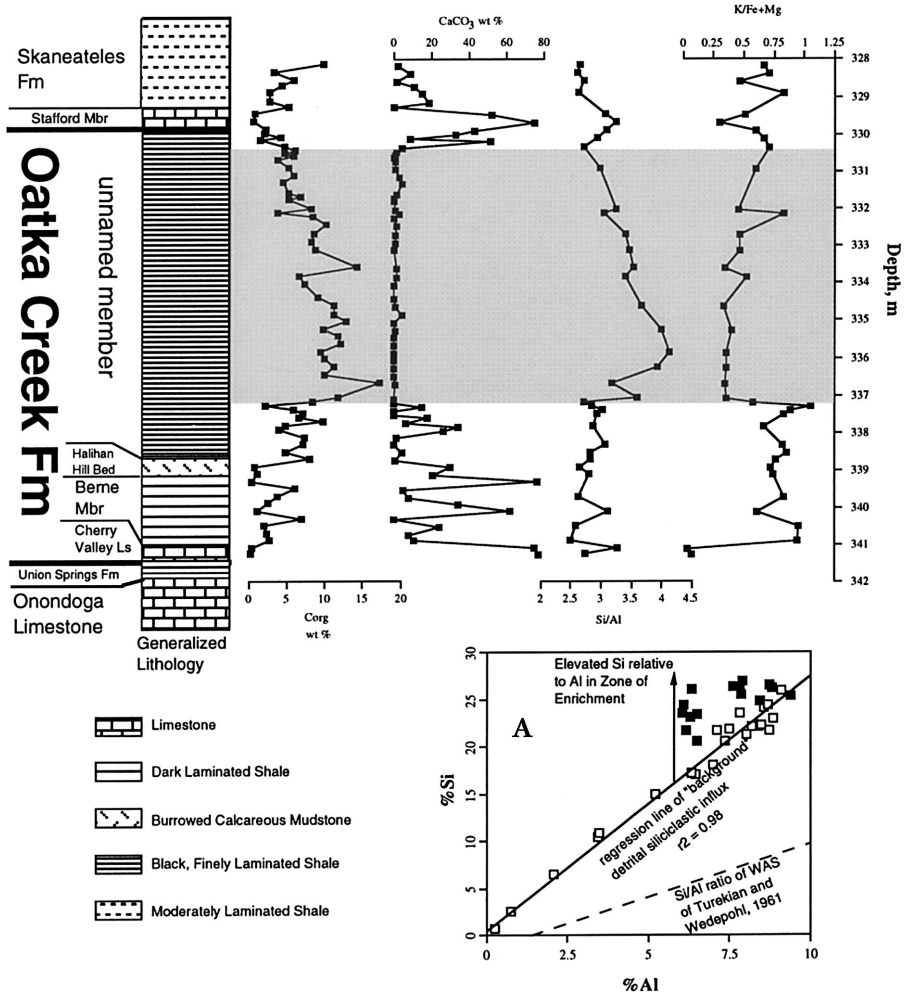

Fig. 4. Depth trends of detrital indicators plotted with C_{org}, $CaCO_3$, and generalized lithostratigraphy. Excursions at the base of the MOE suggest maximum condensation at this horizon. (A) Cross plot of Si versus Al shows enrichment of Si over Al relative to World Average Shale (Turekian and Wedepohl, 1961) and increased enrichment in Si relative to Al in MOE.

more than 200 but does have a generally increasing trend upsection (fig. 6). In the MOE, C_{org}/P_{total} reaches a maximum of almost 400 and then decreases very gradually to values of less than 100 in the overlying Skaneateles Formation. Concentrations of organic phosphorus are below detection throughout the unnamed member. $\delta^{13}C_{org}$ values in the Oatka Creek Formation are quite uniform throughout the section at ~–30 permil with variability of generally <0.5 permil. This uniformity in isotopic values occurs seemingly without regard for variations in lithology or other parameters.

DISCUSSION

Primary Inputs and Dilution Effects

Most sedimentary deposits can be divided geochemically into three major components: (1) a biogenic component composed of OM, $CaCO_3$, and silica derived from

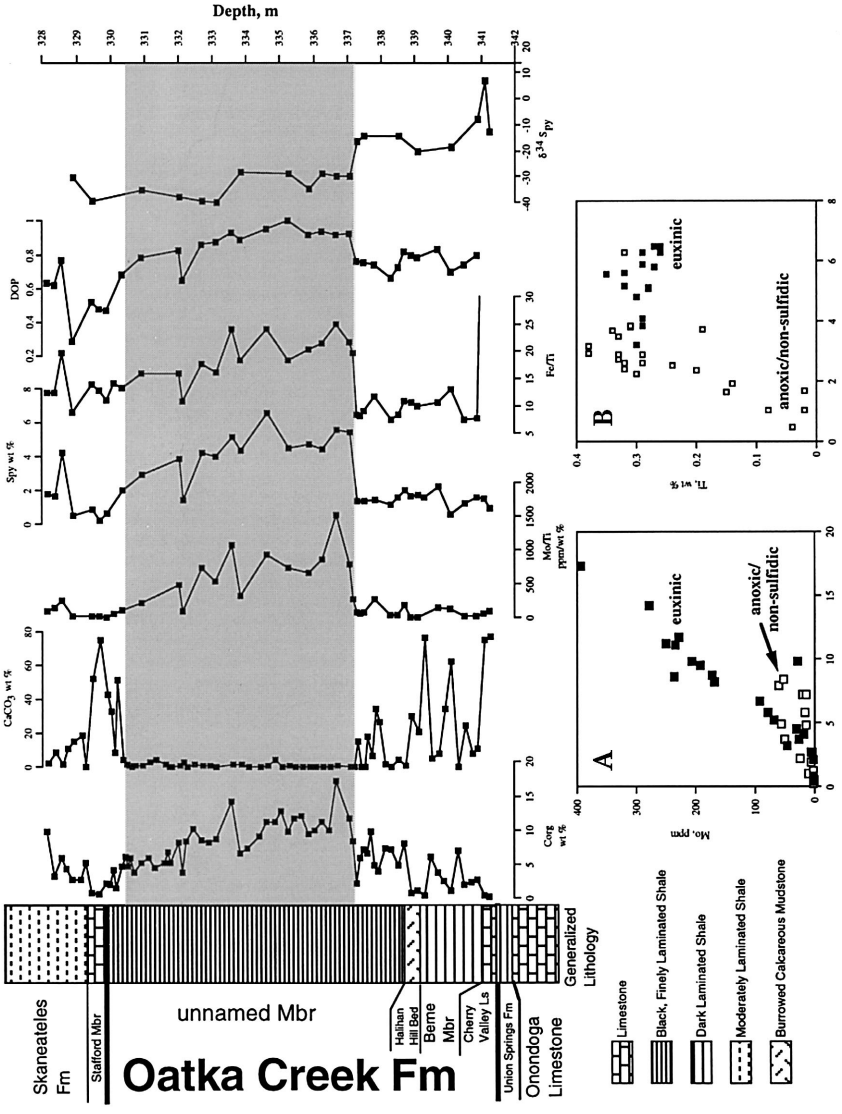

Fig. 5. Depth trends of redox proxies with C_{org}, $CaCO_3$, and generalized lithostratigraphy. All redox proxies indicate the onset of euxinic conditions during deposition of the MOE. (A) Mo versus C_{org}, illustrating coupling of Mo deposition with C_{org} deposition under euxinic conditions; (B) Ti versus Fe, illustrating decoupling of Fe and Ti during deposition of MOE, suggesting enhanced water-column formation of pyrite from dissolved Fe species. In both (A) and (B), black squares represent deposition during MOE, and open squares represent deposition before and after MOE.

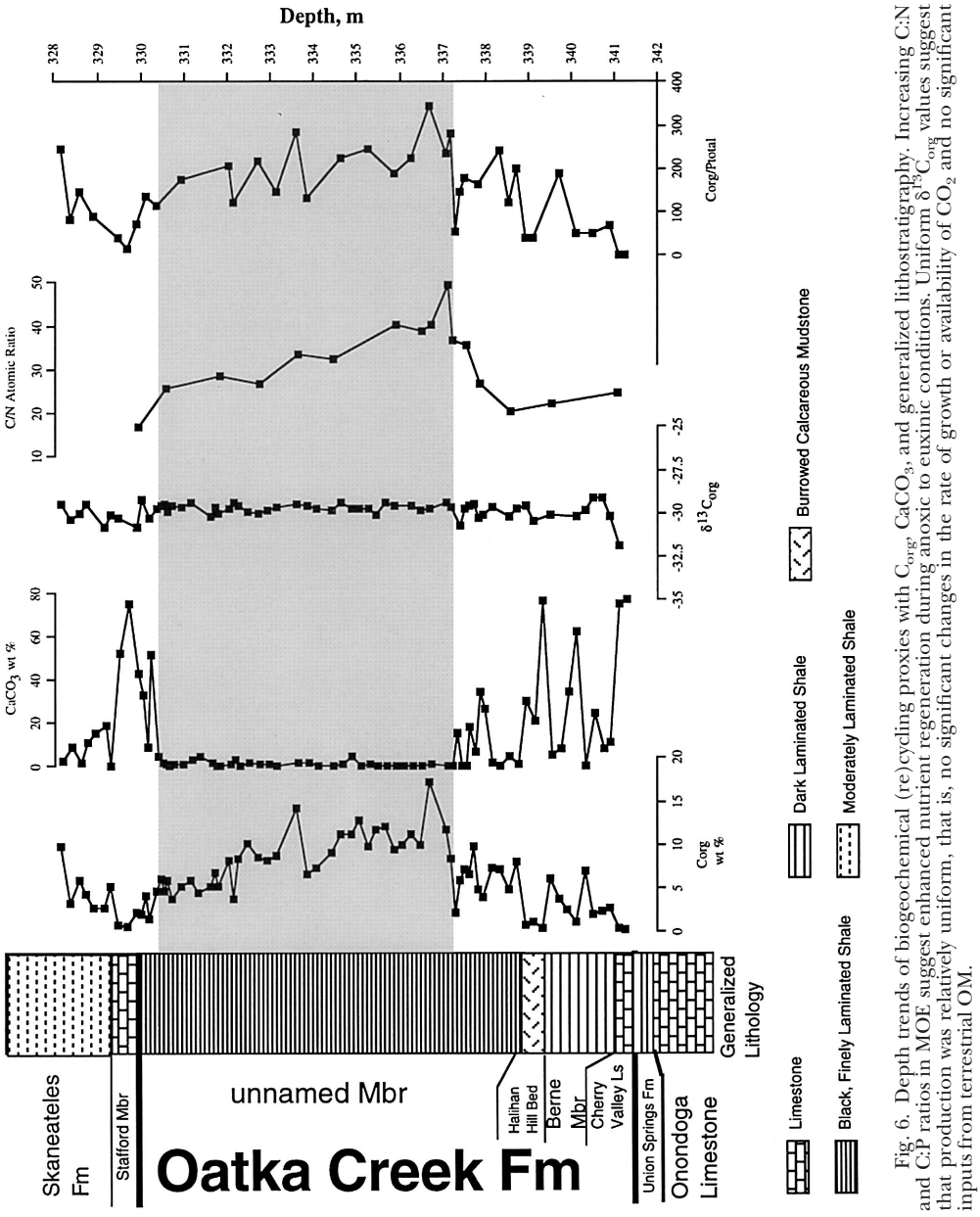

Fig. 6. Depth trends of biogeochemical (re)cycling proxies with C_{org}, $CaCO_3$, and generalized lithostratigraphy. Increasing C:N and C:P ratios in MOE suggest enhanced nutrient regeneration during anoxic to euxinic conditions. Uniform $\delta^{13}C_{org}$ values suggest that production was relatively uniform, that is, no significant changes in the rate of growth or availability of CO_2 and no significant inputs from terrestrial OM.

primary production; (2) a detrital component composed of siliciclastic grains derived from fluvial, eolian, and volcanogenic sources; and (3) an authigenic component composed of redox sensitive trace elements such as Mo, V, and Fe and diagenetically precipitated $CaCO_3$ and silica. Previous studies have determined that this three-component geochemical system is fairly representative of the major inputs to sedimentary systems (Chester and Aston, 1976; Dean and Arthur, 1987, 1998). For example, Dean and Arthur (1998) grouped various elements into these three fundamental geochemical categories: (1) variations in Al, Ti, Na, K, Mg, Ce, Li, Nd, Sc, and Y are dominantly controlled by changes in detrital inputs; (2) variations in Ca, inorganic C ($CaCO_3$), and Sr are controlled by processes involved in the formation and modification of carbonate facies; and (3) variations in Mo, Cd, Cu, Ni, V, and Zn reflect changes in authigenic/diagenetic precipitation controlled mainly by redox state. Bulk C_{org} levels typically correlate strongly with the redox elements, and Fe was found to correlate with both the detrital and redox groupings (Dean and Arthur, 1998).

It can be assumed that each of the three major components will dilute the other two to some degree. In an effort to assess the extent of mutual dilution, we examined cross plots of the major geochemical components (fig. 7). Strong negative correlations are observed between $CaCO_3$ and Al and Si (fig. 7A) and between C_{org} and $CaCO_3$ (fig. 7B), as would be expected given the mutually exclusive depositional mechanisms; however, two trends of major interest are apparent in the plot of Al and Si versus $CaCO_3$ (fig. 7A). At the lowest concentrations of $CaCO_3$ (in the MOE) significant variations in the concentration of both Al and Si are observed, suggesting that factors beside $CaCO_3$ content are influencing the detrital geochemical signature of the deposit at times of minimum carbonate deposition. When Al and Si are plotted against the third primary geochemical parameter, C_{org} (fig. 7C), we see that increases in C_{org} from 0 to about 10 percent are accompanied by increasing Al and Si (although there is much scatter), but that samples with the highest values of C_{org} (which also have the lowest concentrations of $CaCO_3$) show a distinct negative correlation with Al and Si. These data indicate that the dominant diluting component is $CaCO_3$, which ranges from 0 percent to 80 percent of the total rock by mass. Thus, any weight percent data would be strongly affected by the relative percent of $CaCO_3$, which could lead to flawed interpretations. Therefore, ratios of different geochemical parameters should be utilized to normalize for artifacts of dilution resulting from variations in the contributions of major components. More specifically, elemental enrichments and depletions relative to crustal (weathering) contributions are assessed by normalizing the data to detrital proxies such as Al, Ti, and (in the absence of biogenic inputs) Si. These ratios are independent of and thus not masked by temporal trends in the extent of $CaCO_3$ dilution, despite the low absolute concentrations relative to $CaCO_3$.

Siliciclastic Deposition

The ratio K/(Fe+Mg) has been proposed to delineate relative changes in detrital and volcanoclastic inputs in hemipelagic strata (Dean and Arthur, 1998). Pratt (1984) showed in the Cretaceous Greenhorn Formation (Western Interior United States of America) that units with higher concentrations of detrital clastics were associated with higher concentrations of discrete illite and clay-sized quartz and thus have higher K concentrations. Conversely, the clay-sized fractions of units with lower concentrations of clastics were determined to have a higher concentration of mixed layer illite/smectite derived from alteration of volcanic ash (Pratt, 1984) and therefore generally have a higher concentration of Fe+Mg. In the Oatka Creek Formation, there is a significant upsection decrease in the K/(Fe+Mg) ratio at the base of the MOE, which again is not associated with an obvious change in lithofacies (fig. 4). If we assume that the background input of volcanic ash to the Devonian Appalachian Basin during deposition of the Oatka Creek Formation was relatively constant (and low, as there are

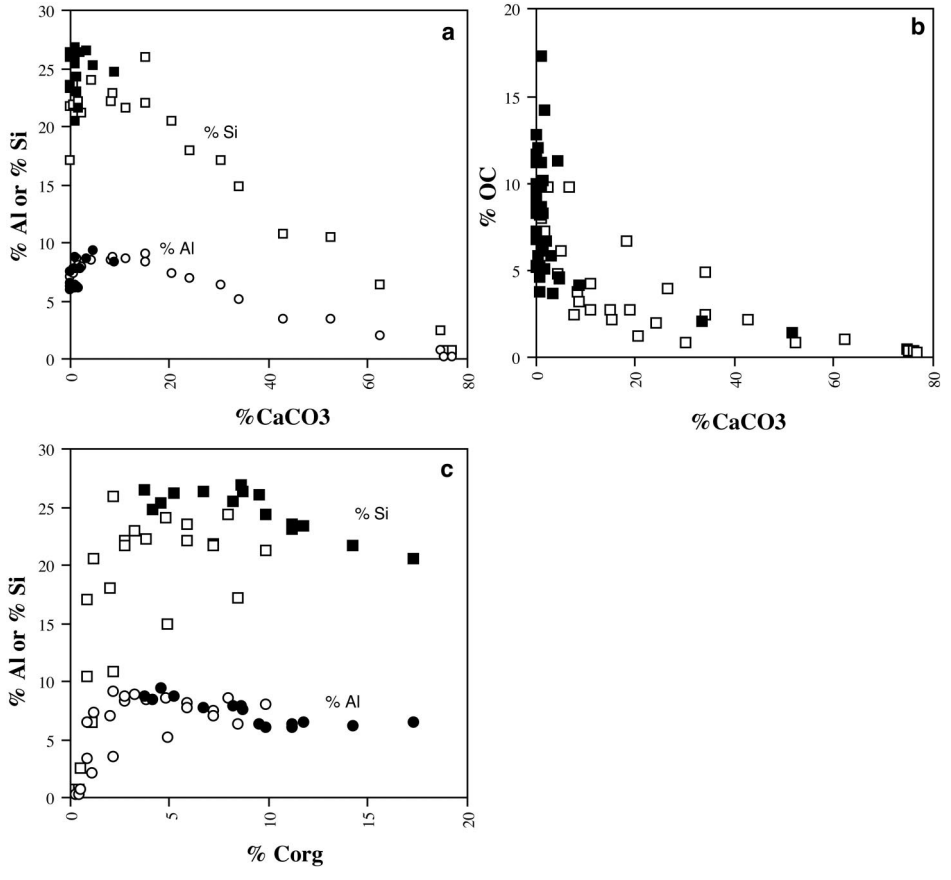

Fig. 7. Cross plots of primary geochemical constituents. In each plot, black symbols represent deposition during MOE, and open symbols represent deposition before and after MOE. (A) $CaCO_3$ versus Al and Si shows effects of $CaCO_3$ dilution on detrital elements. (B) C_{org} versus $CaCO_3$ shows mutual dilution of OM and carbonate. (C) C_{org} versus Al and Si shows slight trend of mutual dilution during MOE deposition but no observable trend during periods of carbonate deposition.

no bentonites in the section), the appreciable decrease in K/(Fe+Mg) suggests one of two things. Either the flux of detrital clastic sediment was significantly reduced relative to the background volcanogenic flux at approx 337 m, making this a highly condensed section, or there was a sudden increase in volcanic activity depositing ash in the basin. Based on the lack of evidence supporting an increase in volcanogenic ash at this time (Ver Straeten, Griffing, and Brett, 1994; Ver Straeten and Brett, 1995; Ver Straeten, 1996), and the existence of other geochemical indicators suggesting increased condensation (such as the Si/Al ratio, see below) we interpret this proxy to indicate maximum condensation at the point of maximum organic carbon concentration (~337 m).

It is possible, however, that changes in the ratio K/(Fe+Mg) reflect multiple processes. For example, although sedimentary Fe accumulation is linked to detrital clays, it is also influenced by the *in situ* formation of iron sulfides such as pyrite, either in the sediments or, under euxinic conditions, in the water column. Thus, changing redox conditions can result in changes in Fe concentrations that are decoupled from variations in detrital or volcanogenic clay input (see details of syngenetic pyrite formation below). In the Oatka Creek Formation the sudden decrease in K/(Fe+Mg)

at 337 m is likely to be at least partially influenced by the onset of euxinic conditions, thereby increasing the deposition of Fe in the form of iron sulfides. In order to test the potential significance of pyrite formation on the K/(Fe+Mg) ratio, we calculated the difference between total Fe and pyrite Fe and used the non-pyrite Fe value to determine the K/(Fe+Mg) ratio. The differences between the curves for K/(Fe+Mg) using the two different pools of iron are insignificant. More importantly, the differences are not well correlated to the interpreted onset of euxinic conditions in the depositional system according to our analysis of independent redox proxies (see below). Nonetheless, because of the potential for multiple Fe sources, we employed additional elemental proxies as supporting evidence of changes in detrital input.

In hemipelagic facies, the Si/Al ratio can provide useful information about detrital versus biogenic sedimentation (Dean and Arthur, 1998). In general, Al in epicontinental mudrocks (like those of the Hamilton Group) is primarily associated with clays derived from fluvial or volcanogenic input (Arthur and others, 1985; Dean and Arthur, 1998). These clays contain Si in proportions determined by their mineralogical composition. XRD analyses of selected discrete samples indicate no major changes in the suite of clay minerals within the mudrocks of the Oatka Creek Formation; therefore, changes in the Si/Al ratio are best interpreted to reflect changes in the Si flux that are independent of the fluvial supply. These changes in the Si flux could include additional biogenic Si associated with increased production of planktonic organisms such as radiolaria or diatom-like organisms (Schieber, Krinsley, and Riciputi, 2000). Alternatively, under appropriate climatic conditions eolian processes will transport quartz silt to basinal depocenters (Lever and McCave, 1983). If this is the case, a marked increase in the Si/Al ratio can reflect either a significant climatic shift (for example, to more arid conditions) or extreme condensation due to a decrease in the fluvial supply relative to a "constant" eolian background flux (which would be typical of basinal settings during transgressive to early highstand systems tracts).

In the Oatka Creek Formation, the Si/Al ratio remains between 2.5 and 3 throughout the lower units. At the onset of organic enrichment, however, it shows a clear increase to values of ~4, followed by a gradual return to the pre-MOE average (fig. 4). As implied above, we believe this trend reflects a decrease in the flux of Al to the basinal depositional system (relative to Si) concurrent with increased burial of OM. A cross-plot of Al versus Si supports this conclusion as samples from above and below the MOE define a clear linear trend (r^2=0.98, fig. 4), which most likely reflects the coupling of Si and Al via deposition of fluvially derived muds. Conversely, samples from the MOE lie above the line of correlation in figure 7, suggesting anomalous Si enrichment. Although we cannot rule out biogenic Si contributions, thin-section analysis suggests that the bulk of the signal is derived from an increase in silt content (fig. 2). In the interval characterized by maximum C_{org} values, quartz silt makes up as much as 40 percent of the mudrock. Under SEM, the silt grains appear angular to subangular with evidence of pitted surface texture, which is consistent with an eolian origin. In addition, the Si/Al ratio in the Oatka Creek Formation is consistently greater than that of the World Average Shale (0.9125, Turekian and Wedepohl, 1961). Because the change in Si/Al corresponds so closely with the increase in C_{org}, as well as other indicators of condensation (such as K/(Fe+Mg), we conclude that the data are best explained by extreme condensation, a process that likely contributed to the enrichment of OM in the Oatka Creek Formation.

Carbonate Deposition

The Oatka Creek Formation is bracketed by limestone beds: the upper boundary by the base of the Stafford Member of the Skaneateles Formation and the lower by the Cherry Valley Limestone, which is the basal member of the Oatka Creek Formation. The other two lower sub-units of the Oatka Creek, the Berne Member (dark laminated

shale) and the Halihan Hill Bed (burrowed calcareous mudstone), are also relatively carbonate-rich. The main sub-unit of the Oatka Creek (the unnamed member), however, is almost completely devoid of carbonate, except for small amounts in the lowermost portion. Two possible explanations exist for the absence of carbonate in this interval. Either the carbonate was never deposited due to exclusion of carbonate producing organisms from the basin and/or reduction of transported detrital carbonate sediment (from the west), or the carbonate was removed through diagenetic remobilization. Hand samples and thin sections show that the little carbonate that exists in the unnamed member is primarily associated with styliolinids. These fossils are extremely thin-shelled yet appear to be as well preserved as those in the overlying and underlying facies, which presumably were deposited under more oxygenated conditions (as indicated by the bioturbation index and macrofossil diversity) and are rich in $CaCO_3$. Thus, there is no direct evidence for the diagenetic removal of carbonate.

The problem of the source of the carbonate (or lack thereof) in the Oatka Creek Formation is critical to understanding the processes that cut-off the supply during deposition of the unnamed member. Carbonate in the Oatka Creek Formation must derive from one, or a combination of three sources: (1) biogenic carbonate, primarily from planktonic organisms such as styliolinids, believed to be pelagic heterotrophs; Yochelson and Lindemann, (1986); (2) detrital carbonate mud brought in from nearby carbonate platforms (such as the Michigan Basin; Fisher and others, 1988; Gutschick and Sandberg, 1991a, b); or (3) authigenically precipitated carbonate. It appears from thin-section analysis that there are contributions from both primary inputs of the styliolinids that lived in the water column and detrital inputs from a carbonate platform environment developed on the Algonquin Arch to the west (Gutschick and Sandberg, 1991a, b). Hinnov, Park, and Erba (2000) proposed a model for deposition of carbonate muds in the Jurassic of the western Tethys (Sogno Formation) that calls upon the redistribution of allodapic muds from shallow carbonate platforms to deep basins during periods of low sealevel. As there is a significant amount of carbonate mud in addition to the styliolinids in the limestones bounding the Oatka Creek Formation, it is possible that an analogous mechanism supplied fine-grained carbonate sediment to the western part of the Appalachian Basin during relative lowstands. Similarly, a correlation of lowstands with bioclastic carbonates accumulation was documented by Brett and Baird (1996) in the overlying Hamilton Group. We therefore propose the following hypothesis to explain both the decrease in allochthonous carbonate as well as the diminution of the styliolinid carbonate. A rapid rise in eustatic sealevel would cause a westward shift of the carbonate facies belt that occupied the western peripheral bulge and cratonic platform or drown it altogether, thus shutting down the supply of transported carbonate sediment from the west. If the relative change in sealevel had been a consequence of tectonism, one might predict uplift of the peripheral bulge and increased shedding of biogenic carbonate to the east.

The reduction but not elimination of styliolinids in the MOE zone of the Oatka Creek suggests ecological exclusion. With so little knowledge of their life habits, it is difficult to have confidence in an interpretation; however, given the evidence for sulfidic conditions in the water column (see below), it is possible that styliolinids were adapted, for at least some portion of their life cycle, to a part of the water column that became inhospitable. The very high concentration of C_{org} through the interval with essentially no carbonate (MOE) indicates that faunal tracking (in other words, lateral migration of organisms to remain in ideal environmental conditions; Brett, Baird, and Miller, 1990) is a more plausible explanation than complete eradication of the planktonic community. The taxa that replaced, displaced, or simply succeeded styliolinids was comprised dominantly of non-calcifying organisms that were living in

portions of the water column not affected by sulfidic conditions (the upper tens of meters).

Depositional Redox Conditions

Black shales of the Devonian Appalachian Basin have long been considered classic examples of stagnant, euxinic basin deposits – based in part on application of the Black Sea as an analog by Byers (1977). Recent work, however, has shown that not all Devonian black shales were deposited under stagnant water-column conditions (Murphy and others, 2000a, b; Murphy, Sageman, and Hollander, 2000; Ingall, Bustin, and Van Cappellen, 1993). Therefore, a goal of this geochemical investigation was to use redox-sensitive elements to determine whether the Oatka Creek Formation was indeed deposited within a stagnant, euxinic setting.

C_{org} concentration is extremely variable, ranging from less than 0.5 percent in some of the limestone beds to more than 17 percent in the black shale facies (fig. 2). Near the base of the unnamed member, the primary black shale facies in the Oatka Creek Formation, there is an excursion in C_{org} content that is independent of any obvious lithologic change. Organic-carbon enrichment is often attributed to a combination of high primary production and enhanced preservation under anaerobic depositional conditions but can be affected significantly by other processes such as variations in detrital sedimentation rate (as summarized in Canfield, 1994). In the Oatka Creek Formation, extreme condensation (as indicated by the siliciclastic proxies) may have contributed significantly to the elevated C_{org} content.

The degree of pyritization (DOP) has been shown to be a reliable indicator of depositional redox conditions in some environments (Raiswell and others, 1988; Jones and Manning, 1994). Values of 0 to 0.45 are considered typical of normal marine (oxygenated) conditions, a range of 0.45 to 0.75 reflects dysoxic to anoxic conditions, and values of 0.75 to 1.0 have been linked to euxinic conditions (Raiswell and others, 1988). Uniformly high DOP values are typically interpreted to indicate deposition under euxinic conditions and suggest that nearly all of the available reactive Fe was utilized in the formation of pyrite (Raiswell and others, 1988; Canfield, Lyons, and Raiswell, 1996; Lyons, 1997). In the Oatka Creek Formation, DOP values range from 0.6 to 1.0 (fig. 5). In the lower units (below the MOE), values are typically 0.6 to 0.8, suggesting episodes of anoxia but dominantly non-sulfidic bottom-waters. At the base of the MOE in the unnamed member, DOP values increase to near 1.0 concomitant with the shift in C_{org} content and generally decrease up section throughout the MOE to roughly pre-MOE values.

Traditional views of DOP invoke exposure time to hydrogen sulfide or depth-dependent variations in the reactivity of the terrigenous Fe flux to explain intrabasinal trends across gradients in depositional redox and across a varying siliciclastic flux under persistent euxinic conditions. It has been shown, however, that DOP can vary by a factor of two across gradients in sedimentation rate beneath a euxinic water-colum (Lyons, 1997). Recent results (Canfield, Lyons, and Raiswell, 1996; Lyons, 1997; Raiswell and Canfield, 1998; Lyons, Werne, and Hollander, 2002) suggest that Fe/Ti ratios and, correspondingly, DOP values can be driven upward by the scavenging of dissolved Fe in sulfidic water columns during syngenetic pyrite formation. Because the scavenged Fe is decoupled from the local terrigenous flux, sediments can become enriched in Fe when terrigenous accumulation is comparatively slow. Along these lines, a cross plot of total Fe versus total Ti suggests covariance between the two in sediments above and below the MOE but a decoupling between the two fluxes within the MOE, suggesting water-column pyrite formation that is at least partially independent of the local siliciclastic sedimentation.

In euxinic settings of more rapid terrigenous deposition, the gradual rainout of scavenged Fe is swamped by continental components, thus yielding Fe/Ti ratios more

typical of oxic or anoxic-nonsulfidic deposition. Similarly, low to intermediate DOP values are observed, which can overlap with those of nonsulfidic settings where the pyrite formation is all diagenetic (within the sediments), and water-column enrichment of the reactive Fe reservoir is not a factor.

In the lower Oatka Creek Formation, DOP and Fe/Ti data (fig. 5) suggest oxic or anoxic but not sulfidic conditions for sediments below the MOE. The rapid increase in both DOP and the Fe/Ti ratio at the base of the MOE and the decoupling between Fe and Ti delivery are consistent with an onset of sulfidic (euxinic) water-column conditions under a comparatively low siliciclastic flux (in other words, condensation). In the presence of syngenetic pyrite formation under euxinic conditions, however, DOP and Fe/Ti values can be more like those of oxic or anoxic-nonsulfidic depositional settings if the scavenged Fe reservoir is overwhelmed by the delivery of Fe coupled to the local siliciclastic flux (Lyons, Werne, and Hollander, 2002). Thus, the up-core decrease in DOP and the Fe/Ti ratio observed in the MOE is consistent with a progressive increase in siliciclastic input above the most condensed horizon at the base of the MOE. This inferred "progressive" increase in siliciclastic input in the MOE is corroborated independently by corresponding decreases in the Si/Al ratio (as discussed above) and by dilution of the observed eolian quartz fraction linked to the Si/Al trends.

As a further test of the redox history of the Oatka Creek Formation, several redox sensitive trace elements were investigated (Mo, Ni, V, Cr, Cd, Cu, Zn). Of these elements, molybdenum appears to be the most effective proxy for the recognition of euxinic depositional conditions. Mo has a very low concentration in seawater, ~10 ppb (Emerson and Huested, 1991), but has been shown to be concentrated in sediments deposited under euxinic conditions (Emerson and Huested, 1991; Helz and others, 1996; Dean, Piper, and Peterson, 1999; Morford and Emerson, 1999). Though the mechanism for Mo enrichment is debated, most consider that Mo is enriched either by inorganic precipitation in H_2S-rich sediments under oxygen-deficient depositional conditions (Emerson and Huested, 1991; Crusius and others, 1996; Zheng and others, 2000; Adelso, Helz, and Miller, 2001) or by scavenging by OM depositing through a sulfidic water-column (Helz and others, 1996; see Lyons, Werne, and Hollander, 2002). The latter mechanism, in particular, requires free H_2S in the water-column for significant Mo enrichment. Piper (1994) suggested that the concentration of Mo in sediments is directly related to the duration of bottom-water sulfidic conditions, and bulk sedimentation rate is also a critical factor in determining the final concentration of Mo in sediments. Interestingly, a low sedimentation rate would not only reduce detrital dilution of Mo and other redox sensitive elements that are scavenged from the water-column but could also promote the continued accumulation of Mo in the sediments for a longer period of time because the sediments would remain in open contact with seawater. Although detrital sources of Mo are generally believed to be negligible, we have normalized Mo concentration to Ti concentration in order to address enrichment beyond crustal levels in the absence of potential diluting effects (in other words, we plot the ratio of Mo/Ti).

In the Oatka Creek Formation, Mo/Ti shifts abruptly from <150 to >1500 at the base of the MOE (fig. 5), suggesting very rapid development of sulfidic conditions in the water column coupled with a decrease in detrital dilution (and a period of maximum open "communication" between bottom waters and pore waters). Mo/Ti gradually declines up section to significantly lower values toward the top of the MOE, eventually reaching a minimum value of <40 in the Stafford Member**.** This up section decrease—as with the Fe/Ti ratios, DOP values, and C_{org} and S_{py} concentrations—supports the hypothesis of progressively increasing clastic

dilution above the condensed zone at the base of the MOE, which is also suggested by the detrital proxies. A cross plot of Mo versus C_{org} suggests a strong coupling between Mo and C_{org} during deposition of the MOE (fig. 5), which may reflect scavenging of Mo by OM descending through a sulfidic water column (Helz and others, 1996; see Lyons, Werne, and Hollander, 2002). The decoupling of C_{org} and Mo in the overlying and underlying units reflects an absence of free sulfide in the water column.

Sulfur isotope systematics have been studied in modern euxinic environments such as the Black Sea (Lyons, 1997). Lyons (1997) determined that pyrite formed in the sediments (diagenetic pyrite) has a more isotopically enriched signature than pyrite formed in the water column (syngenetic pyrite). This difference in $\delta^{34}S_{py}$ between diagenetic and syngenetic pyrite is attributed to formation in a restricted system (sediment pore waters) as opposed to an "open" system with a virtually limitless reservoir of available sulfide in the water column (Lyons 1997). Based on these findings, more-enriched values of $\delta^{34}S_{py}$ would suggest diagenetically formed pyrite, and isotopically depleted pyrite values can be used to identify syngenetic pyrite and therefore euxinic depositional conditions. In the lower Oatka Creek Formation (Berne Member), pyrite sulfur isotope values are relatively enriched, with values near –10 permil, suggesting dominantly diagenetic pyrite formation in oxic or oxygen-deficient but nonsulfidic settings (fig. 5). At the base of the MOE, $\delta^{34}S_{py}$ values decrease abruptly to ~–24 permil and remain between –20 and –35 permil through the remainder of the unit. These comparatively uniform and depleted pyrite sulfur isotope values (relative to a $\delta^{34}S$ value of ~+21 permil for coeval seawater sulfate; Claypool and others, 1980) suggest pyrite formation under "open-system" conditions, such as would exist if pyrite formed in the water column in a euxinic depositional system (Lyons, 1997). Therefore, up-section decreases in Fe/Ti and Mo/Ti ratios, DOP, C_{org}, and S_{py} in the MOE are interpreted to reflect increasing siliciclastic dilution under dominantly euxinic conditions.

Biogeochemical Cycling

Marine primary production is limited by the availability of nutrients, primarily N and P (Broecker and Peng, 1982). Both N and P have been proposed to limit production on geological time scales (Falkowski, 1997; and Broeker and Peng, 1992, respectively). However, a recent model by Tyrell (1999) suggests that P is the more significant limiting nutrient on geological time scales, whereas N is limiting on ecological time scales. It has long been known that marine plankton incorporate N and P into their biomass, along with carbon, in the approximate ratio of 106C:16N:1P (Redfield, Ketchum, and Richards, 1963). Significant increases in the C:N or C:P ratios suggest either variations in OM source (such as marine versus terrestrially dominated OM reservoirs) or preferential release (remineralization) of N and/or P from the sediments to the water column. Although Anderson and Sarmiento (1994) suggested that there is no preferential regeneration of either N or P relative to C under normal marine (that is, oxic) conditions (other than effects associated with denitrification), it has been argued that N is preferentially released under oscillating redox conditions (Aller, 1994) and that P is preferentially released under anoxic conditions (Ingall and Jahnke, 1997; McManus and others, 1997; Anderson, Delaney, and Faul, 2001). Upon release, water column mixing would make these nutrients available for biological utilization, thus increasing the potential delivery of OM to the sediments. Analysis of both N (organic) and P (organic and total), in conjunction with C_{org} determinations, can therefore be used to assess patterns of biogeochemical recycling as they relate to temporal trends in primary production and depositional redox conditions (Ingall and Jahnke, 1997; Murphy and others, 2000). Because remineralized P may be retained as inorganic phosphates in sediments, particularly in anaerobic sediments overlain by

oxygenated bottom waters (Fillipelli, 1997), variations in the C:P ratio in ancient sedimentary deposits should be based upon total P rather than only organic P (Fillipelli, 1997; Anderson, Delaney, and Faul, 2001).

A recently proposed model for black shale deposition called upon many different factors for the inception, maintenance, and termination of black shale deposition in the Geneseo Formation of the Devonian Appalachian Basin (Murphy and others, 2000a,b). The model invoked thermal stratification, rather than salinity-based density stratification, to produce benthic anoxia. Thermal stratification is likely to be a seasonal event and is therefore more plausible geologically than the "permanent pycnocline" of earlier models (Byers, 1977; Ettensohn 1992), especially for a shallow epeiric sea such as the Devonian Appalachian Basin that is potentially mixed by storms on a regular basis. If seasonal thermal stratification is assumed, it is possible that events such as increasing primary productivity and the subsequent increase in the rain of OM to the sediments could increase the intensity and/or duration of seasonal to annual anoxia associated with thermal stratification, thereby leading to increased remineralization of N or P relative to C and initiating a positive feedback between bottom-water oxygen levels and nutrient recycling (Murphy and others, 2000a,b; Murphy, Sageman, and Hollander 2000).

The integrated data set outlined in the above sections is consistent with euxinic conditions for deposition of the MOE. Nevertheless, the gradual increase in the C_{org}/P_{total} ratio (fig. 6) in the lower units of the Oatka Creek Formation suggest an up-section increase in the preferential release of P relative to C that occurs under anoxic conditions (Ingall and Jahnke, 1997). Therefore, this trend may reflect a gradual increase in the intensity and/or duration of anoxic periods induced by thermal stratification. In fact, there is no organic P preserved in the MOE, suggesting the ultimate establishment of dominantly anoxic conditions and that all of the P_{org} was either released back into the water column or remineralized to P_{inorg}. Additional support for the thermal stratification model rather than permanent anoxia, at least for the lower part of the Oatka Creek, is found in the C_{org}/N_{org} ratios (fig. 6). Although the specific processes governing N remineralization are far from being fully understood, recent evidence suggests that N may be preferentially released relative to C during the oxic phase of oscillating oxic-anoxic conditions (Aller, 1994). Thus, the increase in C_{org}/N_{org} ratio going up-section toward the base of the MOE suggests oscillating conditions between oxic and anoxic conditions as manifested in the noisy but generally increasing values of C_{org}/P_{total}. Within the MOE, C_{org}/P_{total} ratios are scattered but consistently high, and the C_{org}/N_{org} decreases up-section, which evokes the predominantly, but perhaps not permanently, euxinic conditions favored by complementary proxy data outlined above.

As mentioned above, variations in C/N/P ratios can be attributed to changes in the source of the OM as well as to preferential release of N and P relative to C. The stable carbon isotope composition of OM ($\delta^{13}C_{org}$) can be utilized to constrain this ambiguity. $\delta^{13}C_{org}$ values are affected by many parameters, including variations in OM type (such as terrestrial or marine), growth rate (Bidigare and others, 1997), $[CO_2]_{aq}$ (Hollander and McKenzie, 1991; Laws and others, 1995), phytoplankton cell geometry (Popp and others, 1998), and OM source (Meyers, 1994). $\delta^{13}C$ values that are invariant through the section, such as those observed in the unnamed member of the Oatka Creek Formation (fig. 6), argue against changes in the character of primary production as a cause for the observed variance in C_{org}/P_{total} and C_{org}/N_{org} relationships. We therefore argue that the variations in C/N/P ratios do indeed represent variations in nutrient regeneration as a function of depositional redox conditions and water column mixing.

SUMMARY AND CONCLUSIONS

The base of the Oatka Creek Formation has been interpreted as being deposited at a time of rapid global eustatic sealevel rise. As sealevel was rising, the depositional environment of the Oatka Creek Formation became increasingly removed from sources of detrital clastics and allodapic muds until at some point (such as the base of the MOE) effectively all the carbonate supply and nearly all detrital sediment were cut off, resulting in an extremely condensed zone. Throughout the period of gradual deepening below the MOE, the basin could have been seasonally anoxic (but likely not sulfidic), with occasional mixing from storm activity. During anoxic periods, P was released preferentially to C, and N was released during the oxic/anoxic oscillations, stimulating primary production in the surface waters. As a result of a combination of extreme sediment starvation (detrital and $CaCO_3$), deepening of the basin (relative sealevel rise), and increasing levels of nutrient regeneration through the positive feedback loop established (nutrient regeneration stimulates production, which increases the supply of OM, and thus increases anoxia and nutrient regeneration still further), the basin became euxinic at 337 m (the base of the MOE).

The onset of euxinic conditions increased the deposition of Mo and S_{py} and increased nutrient regeneration to maximum levels, stimulating maximum rates of OM production. Eventually, as relative sealevel fell, the basin appears to have become euxinic and remained dominantly so through the MOE. Nevertheless, a corresponding increase in the siliciclastic flux progressively diluted the euxinic signal of high Fe/Ti and Mo/Ti ratios, elevated DOP values, and high concentrations of C_{org} and S_{py}, which are manifested most strongly in the condensed interval at the base of the MOE. Finally, as relative sealevel continued to fall, the depositional conditions in the basin may have returned to more "normal" (oxic) marine conditions with the return of carbonate mud deposition from the west by the time of deposition of the overlying Skaneateles Formation.

To summarize, based on the observed relationships among the lithofacies, biofacies, and geochemical proxies analyzed we conclude:

1. Carbonate was a major diluting factor in the basin, and concentrations of the redox-sensitive components were accentuated in the MOE by the absence of calcium carbonate. Carbonate deposition was probably restricted by the relative sealevel rise, which reduced the input of carbonate muds from the platform to the west and facilitated the onset of euxinic conditions, causing styliolinids to migrate to more hospitable conditions (possibly to the east).
2. The base of the MOE within the unnamed member of the Oatka Creek Formation was deposited as a highly condensed section, which is evident from the increase in the relative concentration of Si versus Al, the increase in eolian silt content, the enrichments in ratios such as Mo/Ti and Fe/Ti, and the high concentrations of C_{org} and S_{py}. Progressive increases in siliciclastic input through the MOE are recorded in decreases in these parameters, as well as decreasing Si/Al ratios and eolian quartz silt content.
3. Dominantly euxinic conditions were established at the condensed horizon, probably as a result of eustatic sealevel rise, although oxygen deficiencies (in the absence of free water-column hydrogen sulfide) likely occurred below the MOE.
4. Though euxinic conditions may have been initiated by a relative sealevel rise, the maintenance of euxinic conditions was probably a result of preferential release of P (relative to C) under anoxic conditions and N during the oxic phase of possible oxic/anoxic oscillations, which stimulated high levels of primary production in the surface waters.

ACKNOWLEDGMENTS

We thank C. Ver Straeten for his contributions to our understanding of Devonian stratigraphy, A. Murphy and S. Meyers for stimulating discussions of Devonian geochemistry, and the Akzo-Nobel Company for the donation of core 9455. This work was supported by NSF-EAR-97-25441 to BBS and NSF-EAR-97-25326 and NSF-EAR-98-75961 to TWL. Critical reviews by R. Raiswell and E. Ingall significantly improved the manuscript.

APPENDIX 1

Carbon data for Devonian Oatka Creek Formation

Sample	Depth, meters	TC wt %	IC wt %	C_{org} wt %	$CaCO_3$ wt %	$\delta^{13}C_{org}$	C/N atomic
1075.7+19	328.17	10.13	0.32	9.81	2.21	-29.48	
1075.7+38	328.36	4.47	1.23	3.24	8.49	-30.38	
1075.7+60	328.57	6.05	0.21	5.84	1.45	-30.01	
1075.7+77	328.72	5.84	1.57	4.27	10.84	-29.45	
1075.7+97	328.92	4.87	2.16	2.71	14.92		
1075.7+118	329.14	5.44	2.72	2.72	18.79	-30.82	
1075.7+136	329.28	5.24		5.24		-30.12	
1075.7+156	329.48	8.37	7.57	0.8	52.30	-30.32	
1075.7+175	329.68	11.3	10.81	0.49	74.69		
1075.7+191	329.89	8.35	6.18	2.17	42.70	-30.85	16.72
1075.7+205	330	6.85	4.81	2.04	33.23	-29.22	
1075.7+216	330.1	5.36	1.25	4.11	8.63		
1075.7+226	330.2	8.9	7.48	1.42	51.68	-30.30	
1075.7+241	330.37	5.23	0.67	4.56	4.62	-29.76	
1075.7+250	330.46	6.29	0.2	6.09	1.38	-29.62	
1075.7+258	330.53	4.74	0.12	4.62	0.82	-29.5	25.57
1075.7+264	330.62	5.89	0.06	5.83	0.41	-29.97	
1075.7+276	330.73	3.85	0.11	3.74	0.76	-29.61	
1085.2+17	330.94	5.3	0.11	5.19	0.76	-29.64	
1085.2+37	331.14	6.25	0.41	5.84	2.83	-29.39	
1085.2+57	331.34	5.19	0.66	4.53	4.56		
1085.2+76	331.6	5.35	0.23	5.12	1.58	-30.19	
1085.2+86	331.71	6.81	0	6.81	0	-29.63	
1085.2+97	331.8	5.23	0.02	5.21	0.13	-30.05	28.48
1085.2+116	332.05	8.32	0.11	8.21	0.76	-29.72	
1085.2+125	332.15	4.15	0.47	3.68	3.24	-29.44	
1085.2+136	332.26	8.31	0	8.31	0	-29.57	
1085.2+155	332.46	10.35	0.21	10.14	1.45	-29.96	
1085.2+174	332.72	8.75	0.14	8.61	0.96	-29.99	26.86
1085.2+195	332.92	8.42	0.17	8.25	1.17	-29.87	
1085.2+215	333.12	8.68		8.68	0	-29.69	
1094.6+1	333.59	14.41	0.23	14.18	1.58	-29.49	33.34
1094.8+13	333.85	6.95	0.27	6.68	1.86	-29.61	
1094.8+35	334.06	7.25		7.25	0	-29.77	
1094.8+72	334.43	9.01		9.01	0	-29.85	32.53
1094.8+92	334.63	11.35	0.16	11.19	1.10	-29.43	

APPENDIX 1 (continued)

Carbon data for Devonian Oatka Creek Formation

Sample	Depth, meters	TC wt %	IC wt %	C_{org} wt %	$CaCO_3$ wt %	$\delta^{13}C_{org}$	C/N atomic
1094.8+111	334.86	11.86	0.61	11.25	4.21	-29.79	
1094.8+131	335.05	12.84		12.84	0	-29.74	
1094.8+151	335.26	9.99	0.13	9.86	0.89	-29.76	
1094.8+170	335.46	11.71		11.71	0	-30.15	
1094.8+190	335.67	12.06	0.05	12.01	0.34	-29.37	
1094.8+211	335.87	9.51		9.51	0	-29.58	40.15
1094.8+230	336.06	9.87		9.87	0		
1094.8+250	336.27	11.17		11.17	0	-29.59	
1094.8+270	336.48	9.99	0	9.99	0	-29.88	38.65
1104.6+0	336.69	17.44	0.14	17.3	0.96	-29.73	40.03
1104.6+41	337.09	11.7		11.7	0	-29.41	49.27
1104.6+53	337.2	8.40		8.40	0	-29.70	36.71
1104.6+63	337.3	4.37	2.18	2.19	15.06		
1104.6+73	337.41	5.93	0.06	5.87	0.41	-30.75	
1104.6+83	337.5	7.23	0.05	7.18	0.34	-29.73	35.57
1104.6+93	337.6	9.30	2.65	6.65	18.31	-29.57	
1104.6+103	337.72	10.72	0.98	9.74	6.77	-29.53	
1104.6+117	337.83	9.81	4.92	4.89	33.99	-30.29	26.89
1104.6+124	337.93	7.80	3.84	3.96	26.53	-30.07	
1104.6+144	338.13	7.45	0.22	7.23	1.52	-29.69	
1104.6+164	338.31	7.20		7.20	0		
1104.6+186	338.53	5.43	0.62	4.81	4.28	-30.17	20.32
1104.6+206	338.73	8.10	0.15	7.95	1.03	-29.74	
1104.6+226	338.92	5.18	4.37	0.81	30.19	-29.57	
1104.6+246	339.11	4.15	2.96	1.19	20.45	-30.45	
1104.6+266	339.31	11.38	10.99	0.39	75.94		
1104.6+286	339.51	6.86	0.74	6.12	5.11	-30.14	21.94
1113.9+18	339.71	4.95	1.18	3.77	8.15		
1114.6+16	339.89	7.43	4.95	2.48	34.20		
1114.6+36	340.09	10.05	9.01	1.04	62.25	-30.22	
1114.6+67	340.31	6.86		6.86		-29.83	
1114.6+86	340.5	5.43	3.48	1.95	24.04	-29.16	
1114.6+106	340.71	3.53	1.11	2.42	7.67	-29.12	
1114.6+125	340.87	4.34	1.59	2.75	10.98	-30.19	
1114.6+137	341.09	11.27	10.88	0.39	75.18	-31.9	24.58
1114.6+151	341.24	11.38	11.12	0.26	76.83		

APPENDIX 2

Iron-sulfur-phosphorus data for the Devonian Oatka Creek Formation

Depth	S_{py} wt %	P_{inorg} wt %	P_{total} wt %	P_{org} wt %	HCl-Fe wt %	Py-Fe wt %	DOP	$\delta^{34}S_{py}$ ‰ CDT
328.17	1.77	0.032	0.027	-0.005	1.18	2.03	0.632	
328.36	1.62	0.019	0.024	0.005	1.14	1.858	0.62	
328.57	4.19	0.021	0.021	0	1.48	4.806	0.765	
328.92	0.508	0.014	0.016	0.002	1.44	0.583	0.288	-23.74
329.48	0.871	0.013	0.015	0.002	0.913	0.999	0.522	-32.9
329.68	0.21	0.029	0.023	-0.005	0.263	0.241	0.478	
329.89	0.678	0.02	0.022	0.002	0.869	0.778	0.472	
330.37	2.01	0.017	0.018	0.001	1.06	2.305	0.685	
330.53		0.017		-0.017				
330.94	2.92	0.013	0.017	0.004	0.926	3.349	0.783	-28.93
331.6		0.015		-0.015				
332.05	3.89	0.021	0.026	0.006	0.928	4.461	0.828	-31.2
332.15	1.44	0.015	0.018	0.004	0.887	1.652	0.651	
332.72	4.18	0.024	0.025	0.001	0.785	4.794	0.859	-32.89
333.12	3.97	0.045	0.033	-0.012	0.669	4.553	0.872	-33.56
333.59	5.17	0.037	0.035	-0.002	0.42	5.929	0.934	
333.85	4.39	0.035	0.038	0.003	0.607	5.035	0.892	-21.7
334.63	6.59	0.032	0.027	-0.005	0.362	7.558	0.954	
335.26	4.49					5.15	1	-22.3
335.87	4.72	0.037	0.035	-0.002	0.504	5.413	0.915	-28.21
336.27	4.4	0.032	0.033	0.001	0.35	5.046	0.935	-22.1
336.69	5.54	0.038	0.03	-0.009	0.584	6.354	0.916	-23.2
337.09	5.42	0.035	0.029	-0.007	0.512	6.216	0.924	-23.6
337.2		0.025		-0.025	0.31			
337.3	1.38	0.025	0.029	0.004	0.495	1.583	0.762	-9.9
337.5	1.36	0.03	0.029	-0.001	0.508	1.56	0.754	-7.76
337.83	1.41	0.023	0.019	-0.004	0.572	1.617	0.739	
338.31	1.13	0.028	0.013	-0.015	0.669	1.296	0.66	
338.53	1.57	0.036	0.03	-0.006	0.681	1.801	0.725	-8.1
338.73	1.99	0.033	0.026	-0.007	0.505	2.282	0.819	
338.92	1.63	0.011		-0.011	0.469	1.869	0.799	
339.11	1.7	0.018	0.008	-0.01	0.537	1.95	0.784	-14.06
339.31	1.61	0.019	0.016	-0.003		1.847	1	
339.71	2.22	0.015	0.005	-0.009	0.503	2.546	0.835	
340.09	0.584	0.016	0.015	-0.001	0.296	0.67	0.694	-12
340.5	1.2	0.037	0.029	-0.009	0.49	1.376	0.737	
340.87	1.61	0.031	0.032	0.001	0.47	1.847	0.797	-1.9
341.09	1.5	0.376	0.305	-0.071	0.108	1.72	0.941	13.41
341.24	0.947	0.371	0.299	-0.072	0.207	1.086	0.84	-6.66

APPENDIX 3

Oatka Creek trace element data (ICP)

Depth meters	Na wt %	Mg wt %	Al wt %	Si wt %	P wt %	K wt %	Ca wt %	Sc ppm
328.17	0.35	1.06	8.03	21.3	0.04	3.25	6.83	15.3
328.36	0.42	1.1	8.85	23	0.04	3.51	4.57	18.5
328.57	0.45	1.08	8.17	22.2	0.04	3.46	2.58	16.9
328.92	0.37	1.24	8.39	22.1	0.03	3.44	8.21	17.7
329.48	0.19	0.86	3.43	10.5	0.02	1.44	23.3	8.7
329.68	0.07	0.56	0.76	2.46	0.03	0.32	32.9	2.3
329.89	0.25	0.83	3.49	10.8	0.03	1.5	22.7	7.2
330.1	0.52	1.08	8.44	24.8	0.03	3.44	4.22	16.6
330.37	0.5	1.12	9.39	25.4	0.04	3.56	3.58	22
330.94	0.51	1.06	8.8	26.2	0.03	3.51	0.79	17.5
332.05	0.64	1.09	7.84	25.5	0.04	3.05	0.7	17.4
332.15	0.38	1.05	8.74	26.6	0.03	3.55	4.42	19.2
332.72	0.47	1.01	7.89	26.9	0.04	3.11	0.76	18.3
333.12	0.5	0.93	7.61	26.4	0.06	2.87	1.58	16.7
333.59	0.49	0.91	6.15	21.7	0.05	2.46	2.31	15.4
333.85	0.5	0.92	7.79	26.4	0.05	3.17	1.13	17
334.63	0.51	0.81	6.29	23.1	0.05	2.46	1.12	14.2
335.26	0.44	0.85	6.09	24.4	0.04	2.4	1.18	14.9
335.87	0.79	0.89	6.32	26.1	0.05	2.43	1.12	14.5
336.27	0.56	0.89	6.02	23.6	0.05	2.38	2.37	15.8
336.69	0.6	0.87	6.48	20.6	0.05	2.55	1.12	16.6
337.09	0.61	0.89	6.5	23.4	0.05	2.6	1.39	14.1
337.2	0.65	0.82	6.34	17.2	0.03	2.63	9.93	11.9
337.3	0.62	0.95	9.11	26	0.04	3.9	3.21	16.3
337.41	0.52	1.03	7.82	23.6	0.04	3.21	6.52	15.8
337.5	0.6	1.08	7.47	21.9	0.04	3.09	7.21	15
337.83	0.42	0.8	5.21	14.9	0.03	2.12	16.8	12.5
338.31	0.54	1.05	7.11	21.8	0.03	2.82	8.53	14.1
338.53	0.54	1.15	8.54	24.1	0.04	3.68	4	16.4
338.73	0.59	1.03	8.67	24.4	0.04	3.63	1.66	17.6
338.92	0.61	1.21	6.46	17.1	0.02	2.72	14.4	13
339.11	0.6	1.43	7.37	20.6	0.03	3.23	8.99	13.5
339.71	0.55	0.9	8.47	22.3	0.02	3.66	5.33	15.9
340.09	0.23	0.4	2.08	6.45	0.02	0.89	27.3	4.5
340.5	0.49	0.93	6.99	18	0.04	3.04	10.9	14.7
340.87	0.55	1.12	8.7	21.7	0.04	3.81	5.09	18.9
341.09	0.07	0.51	0.23	0.75	0.3	0.07	34.6	2.1
341.24	0.06	0.26	0.26	0.71	0.34	0.09	34.4	1.3

APPENDIX 3 (continued)

Oatka Creek trace element data (ICP)

Depth meters	Ti wt %	V ppm	Cr ppm	Mn ppm	Fe wt %	Co ppm	Ni ppm	Cu ppm
328.17	0.31	166	77	226	3.81	16	91	117
328.36	0.31	195	98	200	3.84	19	96	110
328.57	0.32	225	103	169	6.29	27	188	233
328.92	0.33	155	149	235	2.91	13	55	59
329.48	0.14	55	13	417	1.95	10	25	21.4
329.68	0.04	12	3	523	0.51	6	5	1.1
329.89	0.15	57	37	437	1.65	8	17	16.2
330.1	0.29	148	91	208	4.09	19	75	127
330.37	0.29	172	55	212	3.87	16	73	118
330.94	0.3	196	98	147	4.8	25	124	136
332.05	0.35	252	75	161	5.56	33	196	152
332.15	0.3	183	98	189	3.22	16	63	67.6
332.72	0.32	331	86	140	5.62	32	239	168
333.12	0.32	277	85	146	5.19	34	186	140
333.59	0.26	382	65	129	6.28	44	295	213
333.85	0.28	275	87	135	5.14	27	146	155
334.63	0.27	328	54	120	6.48	41	261	172
335.26	0.28	337	71	147	5.11	41	255	176
335.87	0.29	310	53	154	5.91	41	237	178
336.27	0.27	363	71	135	5.8	35	238	182
336.69	0.26	421	58	129	6.51	53	349	245
337.09	0.29	383	65	125	6.29	37	271	209
337.2	0.19	210	44	178	3.73	14	93	148
337.3	0.33	204	60	154	2.75	16	71	115
337.41	0.32	150	68	185	2.6	12	66	87.7
337.5	0.29	172	85	199	2.62	13	79	107
337.83	0.2	192	59	252	2.36	11	83	129
338.31	0.32	158	83	216	2.4	24	83	147
338.53	0.38	150	85	186	3.18	29	72	99.4
338.73	0.34	265	101	165	3.68	17	132	187
338.92	0.24	95	58	262	2.54	11	30	18.2
339.11	0.29	108	50	211	2.88	14	34	26.5
339.71	0.33	280	77	140	3.5	20	138	128
340.09	0.08	52	5	216	1.05	6	28	38.7
340.5	0.3	129	80	194	2.24	11	52	30.9
340.87	0.38	198	91	189	2.93	14	73	45.7
341.09	0.02	4	-1	173	1.68	2	4	0.6
341.24	0.02	11	4	265	1.05	3	5	1.2

APPENDIX 3 (continued)

Oatka Creek trace element data (ICP)

Depth meters	Zn ppm	As ppm	Sr ppm	Y ppm	Zr ppm	Mo ppm	Ba ppm	La ppm
328.17	56.6	27	243	20.8	94.1	28	359	31.2
328.36	52.3	31	159	18	109	47	413	32
328.57	66.1	59	160	16.2	116	79	405	31
328.92	47.2	20	229	19.2	93.4	5	394	33
329.48	6.8	14	460	32.2	41.4	2	145	27
329.68	6.3	-3	285	21.9	13.8	1	59	10.8
329.89	28.1	13	375	38.6	48.2	2	149	26.3
330.1	26.7	32	177	20.1	128	18	451	31
330.37	57	32	325	24.7	120	31	235	32.7
330.94	83	43	892	19.3	121	68	200	20
332.05	48.3	38	723	25.7	139	169	130	27
332.15	108	41	202	46.3	114	27	446	46
332.72	55.3	58	122	32.8	111	236	408	37.1
333.12	56.3	55	128	34.8	131	173	332	37
333.59	494	66	116	31.8	119	279	268	31.4
333.85	38.3	48	113	31.5	112	93	367	36.2
334.63	99	70	109	36	92.9	251	305	31.7
335.26	1200	53	102	34.6	115	206	306	32
335.87	135	54	118	30.8	127	192	296	31.6
336.27	147	55	118	34.5	124	234	281	32
336.69	3850	55	88.4	32.5	138	394	272	31
337.09	463	54	101	23.3	113	229	261	29
337.2	52.2	33	205	52.8	102	53	288	38
337.3	3680	25	195	23.4	133	24	399	35.5
337.41	32.7	20	214	27.1	102	16	354	35
337.5	35.2	19	218	26.8	116	20	378	34
337.83	177	11	330	36	86.4	56	230	32
338.31	38.6	14	257	21.7	128	14	284	30
338.53	37.1	21	222	19.2	141	15	358	35
338.73	56.2	23	131	17.8	122	60	384	32.1
338.92	12.5	17	370	19.7	90.7	3	248	30.2
339.11	16.5	24	318	17	104	3	276	30.2
339.71	42.3	27	303	14.5	126	51	333	30.5
340.09	16.6	-3	495	12.4	32.8	11	83	16.4
340.5	12.4	11	256	19	96.3	6	269	32.9
340.87	16.4	22	189	16.6	146	6	364	34.9
341.09	3.1	-3	334	20.7	6.1	1	7	21.7
341.24	17.3	4	311	38.7	4.1	2	9	24.9

References

Adelson, J.M., Helz, G.R., and Miller, C.V., 2001, Reconstructing the rise of recent costal anoxia; molybdenum in Chesapeake Bay sediments: Geochimica et Cosmochimica Acta, v. 65, p. 237–252.

Aller, R.C., 1994, Bioturbation and remineralization of sedimentary organic matter: effects of redox oscillation: Chemical Geology, v. 114, no. 3–4, p. 331–345.

Anderson, L.A., and Sarmiento, J.L., 1994, Redfield ratios of remineralization determined by nutrient data analysis: Global Biogeochemical Cycles, v. 8, no. 1, p. 65–80.

Anderson, L.D., Delaney, M.L., and Faul, K.L., 2001, Carbon to phosphorous ratios in sediments: Implications for nutrient cycling: Global Biogeochemical Cycling, v. 15, p. 65–79.

Arthur, M.A., Dean, W.E., Pollastro, R.M., and Scholle, P.A., 1985, Comparative geochemical and mineralogical studies of two cyclic transgressive pelagic limestone units, Cretaceous Western Interior Basin, U.S., *in* Pratt, L.M., Kauffman, E.G., and Zelt, F.B., editors, Fine-Grained Deposits and Biofacies of the Cretaceous Western Interior Seaway: Evidence of Cyclic Sedimentary Processes, Society for Economic Petrologists and Mineralogists Field Trip Guidebook, v. 4, p. 16–27.

Arthur, M.A., and Sageman, B.B., 1994, Marine black shales: A review of depositional mechanisms and significance of ancient deposits: Annual Reviews in Earth and Planetary Science, v. 22, p. 499–551.

Aspila, K.I., Agemian, H., and Chau, A.S.Y., 1976, A semi-automated method for the determination of inorganic, organic and total phosphate in sediments: Analyst v.101, p. 187–197.

Baird, G.C., and Brett, C.E., 1986, Erosion on an anaerobic seafloor; significance of reworked pyrite deposits from the Devonian of New York State: Palaeogeography, Palaeoclimatology, Palaeoecology, v. 57, no. 4, p. 157–193.

Berner, R.A., 1970, Sedimentary pyrite formation, American Journal of Science, v. 268, p. 1–23.

——— 1984, Sedimentary pyrite formation: An update: Geochimica et Cosmochimica Acta, v. 48, p. 605–615.

Bidigare, R.R., Fluegge, A., Freeman, K.H., Hanson, K.L., Hayes, J.M., Hollander, D.J., Jasper, J.P., King, L.L., Laws, E.A., Milder, J., Millero, F.J., Pancost, R., Popp, B.N., Steinberg, P.A., and Wakeham, S.G., 1997, Consistent fractionation of ^{13}C in nature and in the laboratory: Growth-rate effects in some haptophyte algae: Global Biogeochemical Cycles, v. 11, no. 2, p. 279–292.

Boucot, A.J., Field, M.T., Fletcher, R., Forbes, W.H., Naylor, R.S., and Pavlides, L., 1964, Reconnaissance bedrock geology of the Presque Isle Quadrangle, Maine: Maine State Geological Survey, Quadrangle Mapping Series 2, 123 p.

Brett, C.E., and Baird, G.C., 1994, Depositional sequences, cycles, and foreland basin dynamics in the Late Middle Devonian (Givetian) of the Genesee Valley and western Finger Lakes region, *in* Brett, C.E., and Scatterday, J., editors, New York State Geological Association Annual Meeting 66th, Field Trip Guidebook, p. 505–585.

——— 1995, Coordinated stasis and evolutionary ecology of Silurian to Middle Devonian faunas in the Appalachian Basin, *in* Erwin, D.H., and Anstey, R.L., editors, New Approaches to Speciation in the Fossil Record: New York, Columbia University Press, p. 285–315.

——— 1996, Middle Devonian sedimentary cycles and sequences in the northern Appalachian basin, *in* Witzke, B.J., Ludvigson, G., and Day, J.E., editors, Paleozoic Sequence Stratigraphy: Geological Society America Special Paper 306, p. 213–242.

Brett, C.E., Baird, G.C., and Miller, K.B., 1986, Sedimentary cycles and lateral facies gradients across a Middle Devonian shelf-to-basin ramp: Ludlowville Formation, Cayuga Basin: New York State Geological Association Annual Meeting 58th, Guidebook, p. 81–127.

——— 1990, A temporal hierarchy of paleoecologic processes within a Middle Devonian sea, *in* Miller, William III, editor, Paleocommunity Temporal Dynamics: The Long-Term Development of Multispecies Assemblies, The Paleontological Society, Special Publication 5, p. 178–209.

Brett, C. E., Dick, V. B., and Baird, G. C., 1991, Comparative taphonomy and paleoecology of Middle Devonian dark gray and black shales from Western New York, *in* Landing, E., and Brett, C.E., editors, Dynamic stratigraphy and depositional environments of the Hamilton Group (Middle Devonian) of New York State, Part 2: Albany, New York State Museum, p. 5–36.

Broecker, W.S., and Peng, T.H., 1982, Tracers in the Sea: Palisades, New York, Eldigio Press, 690 p.

Byers, C. W., 1977, Biofacies patterns in euxinic basins: A general model, *in* Cook, H.E., and Enos, P., editors, Deep water carbonate environments, Society of Economic Paleontologists and Mineralogists, p. 5–17.

Canfield, D.E., 1994, Factors influencing organic carbon preservation in marine sediments: Chemical Geology, v. 114, no. 3–4, p. 315–329.

Canfield, D.E., Lyons, T.W., and Raiswell, R., 1996, A model for iron deposition to euxinic Black Sea sediments: American Journal of Science, v. 296, p. 818–834.

Canfield, D.E., Raiswell, R., and Bottrell, S., 1992, The reactivity of sedimentary iron minerals toward sulfide: American Journal of Science, v. 292, p. 659–683.

Canfield, D.E., Raiswell, R., Westrich, J.T., Reaves, C.M., and Berner, R.A., 1986, The use of chromium reduction in the analysis of reduced inorganic sulfur in sediments and shales: Chemical Geology, v. 54, p. 149–155.

Chester, R., and Aston, S.R., 1976, The geochemistry of deep-sea sediments, *in* Riley, J.P., and Chester, R., editors, Chemical Oceanography, v. 6: New York, Academic Press, p. 281–390.

Claypool, G.E., Holser, W.T., Kaplan, I.R., Sakai, H., and Zak, I., 1980, The age curves of sulfur and oxygen isotopes in marine sulfate and their mutual interpretations: Chemical Geology, v. 28, p. 199–260.

Crusius, J., Calvet, S., Pedersen, T., and Sage, D., 1996, Rhenium and molybdenum enrichments in sediments as indicators of oxic, suboxic, and sulfidic conditions of deposition: Earth and Planetary Science Letters, v. 145, p. 65–78.

Dean, W.E., and Arthur, M.A., 1987, Inorganic and organic geochemistry of Eocene to Cretaceous strata recovered from the lower continental rise, North American Basin, site 603, Deep Sea Drilling Project leg 93, *in* van Hinte, J.W., Wise, S.W., and others, editors, Initial Reports of the Deep Sea Drilling Project, Volume XCII, 93: Washington, District of Columbia, p. 1093–1137.

——— 1998, Geochemical expressions of cyclicity in Cretaceous pelagic limestone sequences: Niobrara Formation, Western Interior Seaway, *in* Stratigraphy and Paleoenvironments of the Cretaceous Western Interior Seaway, USA: Society of Economic Paleontologists and Mineralogists Concepts in Sedimentology and Paleontology 6, p. 227–255.

Dean, W.E., Piper, D.Z., and Peterson, L.C., 1999, Molybdenum accumulation in Cariaco basin sediment over the past 24 ky: A record of water-column anoxia and climate: Geology, v. 27, p. 507–510.

Demaison, G.I. and Moore, G.T., 1980, Anoxic marine environments and oil source bed genesis: American Association of Petroleum Geologists, v. 64, p. 1179–1209.

Dennison, J.M., 1985, Catskill Delta shallow marine strata, *in* Woodrow, D. L., and Sevon, W. D, editors, The Catskill Delta: Geological Society of America Special Paper 201, p. 91–106.

Droser, M.L., and Bottjer, D.J., 1986, A semiquantitative field classification of ichnofabric: Journal of Sedimentary Petrology, v. 56, no. 4, p. 558–559.

Emerson, S.R., and Huested, S.S., 1991, Ocean anoxia and the concentrations of molybdenum and vanadium in seawater: Marine Chemistry, v. 34, p. 177–196.

Ettensohn, F.R., 1985a, The Catskill Delta complex and the Acadian Orogeny: A model, *in* Woodrow, D.L., and Sevon, W.D., editors, The Catskill Delta: Geological Society of America Special Paper 201, p. 39–49.

——— 1985b, Controls on development of Catskill Delta complex basin-facies, *in* Woodrow, D.L., and Sevon, W.D., editors, The Catskill Delta: Geological Society of America Special Paper 201, p. 65–77.

——— 1992, Controls on the origin of the Devonian-Mississippian oil and gas shales, east-central United States: Fuel, v. 71, p. 1487–1492.

Ettensohn, F.R., Miller, M.L., Dillman, S.B., Elam, T.D., Geller, K.L., Swager, G,. Markowitz, G.D., Woock, F.D., and Barron, L.S., 1988, Characterization and implications of the Devonian-Mississippian black shale sequence, eastern and central Kentucky, U.S.A.: Pycnoclines, transgression, and tectonism, *in* McMillan, N.J., Embry, A.F., and Glass, D.J., editors, Devonian of the World, II: Canadian Society of Petroleum Geologists Memoir 14, p. 323–345.

Falkowski, P.G., 1997, Evolution of the nitrogen cycle and its influence on the biological sequestration of CO_2 in the ocean: Nature, v. 387, p. 272–275.

Fillipelli, G., 1997, Controls on the phosphorus concentration and accumulation in marine sediments: Marine Geology, v. 139, p. 231–240.

Fisher, J.H., Barratt, M.W., Droste, J.B., and Shaver, R.H., 1988, Michigan Basin, *in* Sloss, L.L., editor, The Geology of North America Volume D-2, Sedimentary Cover-North American craton; U.S.: Boulder, Colorado, Geological Society of America, p. 361–382.

Gutschick, R.C. and Sandberg, C.A., 1991a, Late Devonian history of Michigan Basin, *in* Catacosinos, P.A., and Daniels, P.A., Jr., editors, Early sedimentary evolution of the Michigan Basin: Geological Society of America Special Paper 256, p. 181–202.

——— 1991b, Upper Devonian biostratigraphy of Michigan Basin, *in* Catacosinos, P.A., and P.A. Daniels, Jr., editors, Early sedimentary evolution of the Michigan Basin: Geological Society of America Special Paper 256, p. 155–179.

Hallam, A., 1984, Pre-Quaternary sealevel changes: Annual Reviews in Earth and Planetary Science, v. 12, p. 205–243.

Hamilton-Smith, T., 1993, Stratigraphic effects of the Acadian orogeny in the autochthonous Appalachian basin, *in* Roy, D.C., and Skehan, J.W., editors, The Acadian Orogeny: Recent Studies in New England, Maritime Canada, and the Autochthonous Foreland: Geological Society of America Special Paper 275, p. 153–164.

Heckel, P.H., and Witzke, B.J., 1979, Devonian world paleogeography determined from distribution of carbonates and related lithic paleoclimatic indicators: Paleontological Association Special Paper 23, p. 99–123.

Hedges, J.I., and Keil, R.G., 1995, Sedimentary organic matter preservation: an assessment and speculative synthesis: Marine Chemistry, v. 49, p. 81–115.

Helz, G.R., Miller, C.V., Charnock, J.M., Mosselmans, J.F.W., Pattrick, R.A.D., Garner, C.D., and Vaughan, D.J., 1996, Mechanism of molybdenum removal from the sea and its concentration in black shales: EXAFS evidence: Geochimica et Cosmochimica Acta, v. 60, no. 19, p. 3631–3642.

Hinnov, L., Park, J., and Erba, E., 2000, A 15 million year long Liassic-Dogger sequence of high frequency rhythmites from the Lombard Basin: A record of orbitally-forced cycles modulated by long term secular environmental changes in West Tethys, *in* Hall, R.L., and Smith, P.L., editors, Advances in Jurassic Research 2000: GeoResearch Forum, v. 6: Zurich, Switzerland, transTech Publications, p. 427–436.

Hollander, D.J., and McKenzie, J.A., 1991, CO_2 control on carbon-isotope fractionation during aqueous photosynthesis: A paleo-pCO_2 barometer: Geology, v. 19, p. 929–932.

House, M.R., 1978, Devonian ammonoids from the Appalachians and their bearing on international zonation and correlations: Special Papers in Palaeontology, v. 21, 70 p.

——— 1981, Lower and Middle Devonian goniatite biostratigraphy, *in* Oliver, W.A. Jr., and Klapper, G., editors, Devonian Biostratigraphy of New York, Part 1: International Union of Geological Sciences, Subcommission on Devonian Stratigraphy, p. 33–37.

House, M.R., and Kirchgasser, W.T., 1993, Devonian goniatite biostratigraphy and timing of facies movements in the Frasnian of eastern North America, *in* Hailwood, E.A., and Kidd, R.B., editors, High Resolution Stratigraphy: Geological Society Special Publication 70, London, p. 267–292.

Ingall, E.D., Bustin, R.M., Van Cappellen, P., 1993, Influence of water column anoxia on the burial and preservation of carbon and phosphorus in marine shales: Geochimica et Cosmochimica Acta, v. 57, no. 2, p. 303–316.

Ingall, E.D., and Jahnke, R., 1997, Influence of water-column anoxia on the elemental fractionation of carbon and phosphorus during sediment diagenesis: Marine Geology, v.139, p. 219–229.

Johnson, J.G., 1971, A quantitative approach to faunal province analysis: American Journal of Science, v. 270, p. 257–280.

Johnson, J. G., and Sandberg, C. A., 1988, Devonian eustatic events in the western United States and their biostratigraphic responses, *in* McMillan, N.J., Embry, A.F., and Glass, D.J., editors, Devonian of the World, III: Calgary, Alberta, Canadian Society of Petroleum Geologists Memoir 14, p. 171–178.

Jones, B., and Manning, D.A.C., 1994, Comparison of geochemical indices used for the interpretation of palaeoredox conditions in ancient mudstones: Chemical Geology, v. 111, p. 111–129.

Kirchgasser, W.T., and Oliver, W.A. Jr., 1993, Correlation of stage boundaries in the Appalachian Devonian, eastern United States: Subcommission on Devonian Stratigraphy: Newsletter, v. 10, p. 5–8.

Klapper, G., 1971, Sequence within the conodont genus Polygnathus in the New York lower Middle Devonian: Geologica et Palaeontologica, v. 5, p. 59–79.

——— 1981, Review of New York Devonian conodont biostratigraphy, *in* Oliver, W. A. Jr., and Klapper, G., editors, Devonian Biostratigraphy of New York, Pt. 1: Washington, District of Columbia, International Union of Geological Sciences, Subcommission on Devonian Stratigraphy, p. 57–66.

Klapper, G., and Johnson, J.G., 1990, Endemism and dispersal of Devonian conodonts: Journal of Paleontology, v. 54, p. 400–455.

Laws, E.A., Popp, B.N., Bidigare, R.R., Kennicutt, M.C., and Macko, S.A., 1995, Dependence of phytoplankton carbon isotopic composition on growth rate and $[CO_2]_{aq}$: Theoretical considerations and experimental results: Geochimica et Cosmochimica Acta, v. 59, p. 1131–1138.

Lever, A., and McCave, I.N., 1983, Eolian components in Cretaceous and Tertiary North Atlantic sediments: Journal of Sedimentary Petrology, v. 53, p. 811–832.

Lichte, F.E., Golightly, D.W., and Lamothe, P.J., 1987, Inductively Coupled Plasma-Atomic Emission Spectrometry, *in* Baedecker, P.A., editor, Methods for geochemical analysis: United States Geological Survey Bulletin 1770, p. B1-B10.

Lyons, T.W., 1997, Sulfur isotopic trends and pathways of iron sulfide formation in upper Holocene sediments of the anoxic Black Sea: Geochimica et Cosmochimica Acta, v. 61, p. 3367–3382.

Lyons, T.W., Werne, J.P., and Hollander, D.J., *in press*, Contrasting sulfur geochemistry and Fe/Al and Mo/Al ratios across the last oxic-to-anoxic transition in the Cariaco Basin, Venezuela: Chemical Geology, *in press*.

McCollum, L.B., 1988, A shallow epeiric sea interpretation for an offshore Middle Devonian black shale facies in eastern North America, *in* McMillan, N.J., Embry, A.F., and Glass, D.J., editors, Devonian of the World II: Canadian Society of Petroleum Geologists Memoir 14, p. 347–355.

McManus, J., Berelson, W.M., Coale, K.H., Johnson, K.S., and Kilgore, T.E., 1997, Phosphorus regeneration in continental margin sediments: Geochimica et Cosmochimica Acta, v. 61, p. 2891–2907.

Meyers, P.A., 1994, Preservation of elemental and isotopic source identification of sedimentary organic matter: Chemical Geology, v. 114, p. 289–302.

Morford, J.L., and Emerson, S.R., 1999, The geochemistry of redox sensitive trace metals in sediments: Geochimica et Cosmochimica Acta, v. 63, p. 1735–1750.

Murphy, A.E., Sageman, B.B., and Hollander, D.J., 2000, Eutrophication by decoupling of the marine biogeochemical cycles of C, N, and P: A mechanism for the Late Devonian mass extinction, Geology, v. 28, p. 427–430.

Murphy, A.E., Sageman, B.B., Hollander, D.J., Lyons, T.W., and Brett, C.E., 2000a, Black shale deposition in the Devonian Appalachian Basin: Siliciclastic starvation, episodic water-column mixing, and efficient recycling of biolimiting nutrients: Paleoceanography, v. 15, no. 3, p. 280–291.

Murphy, A.E., Sageman, B.B., Ver Straeten, C.A., and Hollander, D.J., 2000b, Organic carbon burial and faunal dynamics in the Appalachian basin during the Devonian (Givetian-Famennian) greenhouse: An integrated paleoecological and biogeochemical approach, *in* Huber, B.T., MacLeod, K.G., and Wing, S.L., editors, Warm Climates in Earth History: Cambridge, United Kingdom, Cambridge University Press, p. 351–385.

Newton, R.J., Bottrell, S.H., Dean, S.P., Hatfield, D., and Raiswell, R., 1995, An evaluation of the use of the chromous chloride reduction method for isotopic analyses of pyrite in rocks and sediment: Chemical Geology (Isotope Geoscience Section), v. 125, p. 317–320.

Pedersen, T.F., and Calvert, S.E., 1990, Anoxia vs. productivity: What controls the formation of organic-carbon-rich sediments and sedimentary rocks?: American Association of Petroleum Geologists Bulletin, v. 74, p. 454–466.

Piper, D.Z., 1994, Seawater as the source of minor elements in black shales, phosphorites and other sedimentary rocks: Chemical Geology, v. 114, p. 95–114.

Popp, B.N., Laws, E.A., Bidigare, R.R., Dore, J.E., Hanson, K.L., and Wakeham, S.G., 1998, Effect of phytoplankton cell geometry on carbon isotopic fractionation: Geochimica et Cosmochimica Acta, v. 62, no. 1, p. 69–77.

Pratt, L.M., 1984, Influence of paleoenvironmental factors on preservation of organic matter in the Middle Cretaceous Green Formation, Pueblo, CO.: American Association of Petroleum Geologists Bulletin, v. 68, p. 1146–1159.

Prave, A.R., Duke, W.L., and Slattery, W., 1996, A depositional model for storm- and tide-influenced prograding siliciclastic shorelines from the Middle Devonian of the central Appalachian foreland basin USA: Sedimentology, v. 43, p. 611–629.

Quinlan, G.M., and Beaumont, C., 1984, Appalachian thrusting and the Paleozoic stratigraphy of the eastern interior of North America: Canadian Journal of Earth Science, v. 21, p. 973–994.
Raiswell, R., Buckley, F., Berner, R.A., and Anderson, T.F., 1988, Degree of pyritization of iron as a paleoenvironmental indicator of bottom water oxygenation, Journal of Sedimentary Petrology, v. 58, no. 5, p. 812–819.
Raiswell, R., and Canfield, D.C., 1996, Rates of reaction between silicate iron and dissolved sulfide in Peru Margin sediments, Geochimica et Cosmochimica Acta, v. 60, p. 2777–2878.
Raiswell, R., and Canfield, D.C., 1998, Sources of iron for pyrite formation in marine sediments: American Journal of Science, v. 298, p. 219–245.
Raiswell, R., Canfield, D.E., and Berner, R.A., 1994, A comparison of iron extraction methods for the determination of degree of pyritisation and the recognition of iron-limited pyrite formation: Chemical Geology, v. 111, p. 101–111.
Redfield, A.C., Ketchum, B.H., and Richards, F.A., 1963, The influence of organisms on the composition of seawater, *in* Hill, M.N., editor, The Sea: v. 2, New York, Interscience Press, p. 26–77.
Rickard, L.V., 1984, Correlation of the subsurface Lower and middle Devonian of the Lake Erie Region: Geological Society of America Bulletin, v. 95, p. 814–828.
Rodgers, John, 1967, Chronology of tectonic movements in the Appalachian region of eastern North America: American Journal of Science, v. 265, p. 408–427.
Schieber, J., Krinsley, D., and Riciputi, L., 2000, Diagenetic origin of quartz silt in mudstones and implications for silica cycling: Nature, v. 406, p. 981–985.
Scotese, C.R., Barrett, S.F., and Van der Voo, R., 1985, Silurian and Devonian base maps: Philosophical Transactions of the Royal Society, London, v. B 309, p. 57–77.
Scotese, C.R., and McKerrow, W.S., 1990, Revised world maps and introduction, *in* McKerrow, W.S., and Scotese, C.R., editors, Paleozoic paleogeography and biogeography: Geological Society Memoir 12, London, p. 1–21.
Slingerland, R., and Loulé, J.-P., 1988, Wind/wave and tidal processes along the Upper Devonian Catskill shoreline in Pennsylvania, U.S.A., *in* McMillan, N.J., Embry, A.F., and Glass, D.J., editors, Devonian of the World, Volume II: Sedimentation: Calgary, Canadian Society of Petroleum Geologists, p. 125–138.
Stookey, L.L., 1970, Ferrozine- A new spectrophotometric reagent for iron: Analytical Chemistry, v. 42, p. 779–781.
Turekian, K.K., and Wedepohl, K.H., 1961, Distribution of the elements in some major units of the earth's crust, Geological Society of America Bulletin, v. 72, p. 175–192.
Tyrrell, T., 1999, The relative influences of nitrogen and phosphorus on oceanic primary production: Nature, v. 400, p. 525–531.
Tyson, R.V., and Pearson, T.H., 1991, Modern and ancient continental shelf anoxia: An overview, *in* Tyson, R.V., and Pearson, T.H., editors, Modern and Ancient continental Shelf Anoxia: Geological Society Special Publication 58, p. 1–24.
Ver Straeten, C.A., ms, 1996, Stratigraphic Synthesis and Tectonic and Sequence Stratigraphic Framework, upper Lower and Middle Devonian, Northern and Central Appalachian Basin: Ph.D. thesis, University of Rochester, 800 p.
Ver Straeten, C.A., and Brett, C.E., 1995, Lower and Middle Devonian foreland basin fill in the Catskill Front: Stratigraphic synthesis, sequence stratigraphy, and the Acadian Orogeny, *in* Garver, J.I., and Smith, J.A., editors, New York State Geological Association: Annual Meeting, 67th Field Trip Guidebook, p. 313–356.
Ver Straeten, C.A., Griffing, D.H., and Brett, C.E., 1994, The lower part of the Middle Devonian Marcellus "Shale", central to western New York state: Stratigraphy and depositional history, *in* Brett, C.E. and Scatterday, J., editors, New York State Geological Association, Annual Meeting, 66th Field Trip Guidebook, p. 270–321.
Witzke, B.J., and Heckel, P.H., 1988, Paleoclimatic indicators and inferred Devonian paleolatitudes of Euramerica, *in* McMillan, N.J., Embry, A. F., and Glass, D. J., editors, Devonian of the World, I: Canadian Society of Petroleum Geologists, Memoir 14, p. 49–63.
Witzke, B.J., 1990, Paleoclimatic constraints for Paleozoic paleolatitudes of Laurentia and Euramerica, *in* McKerrow, W.S., and Scotese, C.R., editors, Paleozoic paleogeography and biogeography: Geological Society Memoir 12, p. 57–74.
Woodrow, D. L., 1985, Paleogeography, paleoclimate, and sedimentary processes of the Late Devonian Catskill Delta, *in* Woodrow, D. L., and Sevon, W. D., editors, The Catskill Delta: Geological Society of America Special Paper 201, p. 51–63.
Woodrow, D. L., Dennison, J. M., Ettensohn, F. R., Sevon, W. T., and Kirchgasser, W. T., 1988, Middle and Upper Devonian stratigraphy and paleogeography of the central and southern Appalachians and eastern Midcontinent, U.S.A, *in* McMillan, N.J., Embry, A. F., and Glass, D. J., editors, Devonian of the World, I: Canadian Society of Petroleum Geologists, Memoir 14, p. 277–301.
Woodrow, D.L., Fletcher, F.W., and Ahrnsbrak, W.F., 1973, Paleogeography and paleoclimate at the depositional sites of the Devonian Catskill and Old Red Facies: Geological Society of America Bulletin, v. 84, p. 3051–3064.
Yochelson, E.L. and Lindemann, R.H., 1986, Considerations on the systematic placement of the Styliolines (*incertae sedis*: Devonian), *in* Hoffman, A., and Niteci, M.H., editors, Problematic Fossil Taxa: Oxford Monographs in Geology and Geophysics 5, Oxford, Oxford University Press, p. 45–48.
Zheng, Y., Anderson, R.F., van Geen, A., and Kuwabara J., 2000, Authigenic molybdenum formation in marine sediments: A link to pore water sulfide in the Santa Barbara Basin. Geochimica et Cosmochimica Acta, v. 64, p. 4165–4178.